DOI:10.14753/SE.2023.2872

Lyophilization: a novel sample preprocessing method to improve the quantitative evaluation of tissue fibrosis

PhD thesis

Tamás Lakat

Károly Rácz Doctoral School of Clinical Medicine

Semmelweis University

Supervisor: Ádám Hosszú, Ph.D,

Official reviewers: Gábor Kökény, MD, Ph.D
Szilveszter Dolgos, MD, Ph.D

Head of the Complex Examination Committee: György Reusz, MD, DSc.

Members of the Complex Examination Committee: Gábor Varga, MD, DSc.
András Folyovich, MD, Ph.D

Budapest
2023

DOI:10.14753/SE.2023.2872

Table of contents

List of abbreviations

ACE – angiotensin converting enzyme

AGEs – advanced glycation end products

AKI – acute kidney injury

Akt – protein-kinase B

AngII – angiotensin-II

ARB – angiotensin receptor blockers

C3M – MMP9 mediated degradation product of type III collagen

Ca – calcium

CKD – chronic kidney disease

CPP – Critical Process Parameters

CTGF – connective tissue growth factor

DKD – diabetic kidney disease

DM – diabetes mellitus

ECM – extracellular matrix

eNOS – endothelial nitric-oxide synthase

ESRD – end-stage renal disease

FDA – US Food and Drug Administration

GAPDH – glyceraldehyde 3-phosphate dehydrogenase

GBD – Global Burden of Disease

GFR – glomerular filtration rate

HPLC-MS – high performance liquid chromatography – mass spectrometry

IR – ischemia/reperfusion

MMP9 – matrix metalloproteinase-9

NFκB – nuclear factor κB

NGAL – Neutrophil gelatinase-associated lipocalin

PAI-1 – plasminogen activator inhibitor-1

PAT – Process Analytical Technology

PDE – peritoneal dialysis effluent

Phos – phosphorous

PKC – protein kinase C

PTH – parathyroid hormone

QbD – Quality by Design

RAAS – renin-angiotensin-aldosterone system

RAASi – RAAS inhibitor

RONS – reactive oxygen and nitrogen species

rPRO-C3 – N-terminal pro-peptide of rodent type III collagen

SGLT2i – sodium-glucose cotransporter 2 inhibitor

STZ – streptozotocin

T_c – collapse temperature

T_e **–** eutectic temperature

T_g **–** glass transition temperature

TGF-ß – transforming growth factor-beta

TUM – tumstatin

TUNEL – terminal deoxynucleotidyl transferase dUTP nick end labeling

uC3M – urinary MMP9 mediated degradation product of type III collagen

αSMA – alpha smooth muscle actin

DOI:10.14753/SE.2023.2872

1. Introduction

1.1. Chronic kidney disease

Chronic kidney disease (CKD) is one of the most prominent cause of mortality and morbidity worldwide. It is defined by the presence of decreasing renal function, excessive albuminuria or both. CKD is a progressive condition which may eventually lead to end-stage renal disease (ESRD) associated with irreversible renal decline. Currently, the only available treatment is renal replacement therapy, mainly dialysis. However, it significantly impairs the quality of patient's life, moreover, it also places a huge burden on the economy and society. Permanent improvement can only be achieved through kidney transplantation, which has remarkable benefits in comparison with the costly dialysis, however, transplant waiting lists are limitless and continuously growing.

1.1.1. Epidemiology

More than 840 million people are struggling with CKD (**Figure 1)**, moreover, its prevalence increases by ~10% each year (1). In the last 30 years, the mortality rate of CKD and ESRD increased by ~40%, thus related deaths account for 4.6% of the overall mortality. Pooled results of 33 population-based representative studies revealed that numerous characteristics have an influence on prevalence values, such as age, sex, race and geographic regions. It has been shown that CKD is more common among women (11.8% *vs.* 10.4%), and the prevalence is higher in low- and middle income countries (10.6-12.5%) (2). According to the Global Burden of Disease (GBD) study database, around 14% of the population is involved in Hungary with a mortality rate of 1.27% (3).

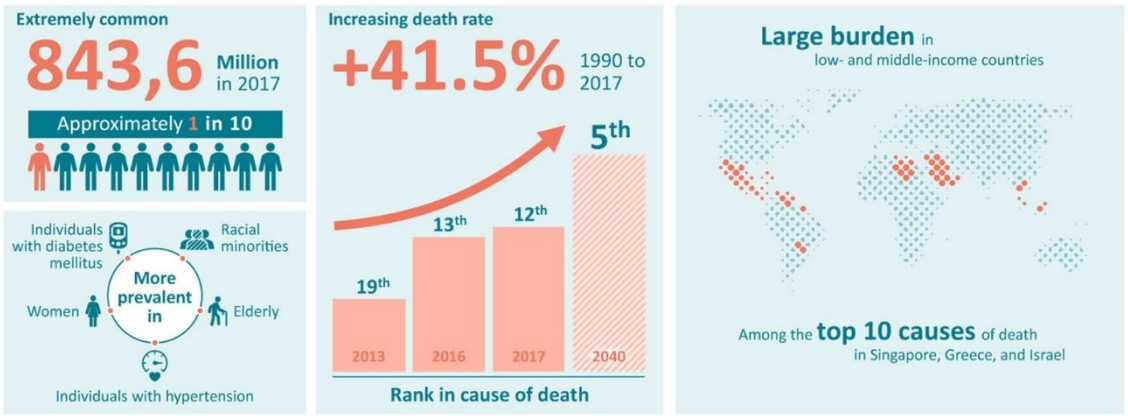

Figure 1. Global statistics of chronic kidney disease (1)

The risk factors for CKD can be stage-wisely grouped as follows: (1) susceptibility factors (family, age, income, etc.), (2) initiation factors (high blood pressure, diabetes, infection, toxicity, autoimmune diseases), (3) progression factors (smoking, uncontrolled hypertension and hyperglycemia), (4) end-stage factors (inappropriate referral or dialysis, temporary vascular access).

1.1.2. Diabetic kidney disease

The kidney is highly sensitive to microvascular damage caused by excessive blood glucose levels and high blood pressure, thereby diabetes mellitus (DM) is presumably one of the leading causes of CKD (4). Almost 50% of the patients with type 2 DM and ~30% with type 1 DM will develop CKD with time (5,6). Consequently, CKD management of patient with DM is a key objective to slow down its progression, which includes controlling hyperglycemia and also blood pressure.

Hyperglycemia is the primal causative factor of DM, which plays essential role in the pathogenesis of diabetic kidney disease (DKD). Chronically increased glucose uptake by tubular epithelial cells results altered protein and lipid structures, oxidative stress and the activation of alternative pathways (7,8). Due to the increased rate of glycolysis, hyperpolarized mitochondria produce excessive levels of reactive oxygen and nitrogen species (RONS), which leads to further cellular damage (9). Hyperglycemia also provokes the production of glycated proteins and lipids called advanced glycation end products (AGEs) (10). These molecules trigger the expression of nuclear factor κB (NFκB), protein kinase C (PKC), and also affect cellular function and structure (11–13). Upregulation of these pathways leads to the activation of macrophages and results increased release of proinflammatory cytokines, transforming growth factor-beta (TGF-ß). and plasminogen activator inhibitor-1 (PAI-1), eventuating extracellular matrix (ECM) deposition, glomerulosclerosis and tubulointerstitial fibrosis (14).

In addition, chronic hyperglycemia increases the expression of angiotensin II (Ang II) and its receptors, resulting in abnormal activation of renin-angiotensin-aldosterone system (RAAS). Overactivation of RAAS mediate vasoconstriction and increase extracellular volume, leading to severe hemodynamic changes including systemic and intraglomerular hypertension, glomerular hyperperfusion and hyperfiltration (15). These

mechanisms are accountable for structural changes in the glomeruli, and initiates the development of DKD. Consequently, patients present albuminuria and decreased glomerular filtration rate (GFR) (16,17).

The theory of chronic hypoxia originates from 1998. *Fine et al.* hypothesized, that glomerular injury leads to decreased postglomerular flow, culminating in peritubular capillary loss (18). Insufficient renal blood flow generates a hypoxic environment, which harmfully affects adjacent capillaries. By the time this hypothesis was confirmed by several *in vivo* experiments, moreover, biopsies taken from CKD patients also showed reduced capillary density (19–21). Persistently decreased blood supply leads to chronic hypoxia, which is the cornerstone of CKD. Proximal tubular cells are particularly vulnerable to hypoxic conditions due to their high oxygen demand and physiologically limited blood supply (22). In DKD, tubular epithelial cells play a key role in the manifestation of renal inflammation and tubulointerstitial fibrosis by releasing profibrotic and proinflammatory cytokines (23,24). Accumulation of fibrotic tissue will further compromise tubular vascularity, thereby maintaining hypoxic environment, which leads to further epithelial cell damage and fibrosis (25,26).

The diagnosis of DKD generally relies on the presence of albuminuria and decreased GFR. However, emerging number of cases report decreased kidney function in the absence of proteinuria in type 2 DM patients (27). Currently, histological investigation is still the most accurate diagnostic approach of DKD, however, renal biopsy is not routinely indicated. Early detection is crucial to effectively slow down DKD progression, thereby, there is a great need for sensitive biomarkers.

The formation and degradation of ECM components lead to specific pro-collagen terminal fragments and protein neo-epitopes secreted into urine, which have recently been discovered as novel, early urinary biomarkers of renal fibrosis (28). Two of them are neo-epitopes of matrix metalloproteinase-9 (MMP-9)-mediated degradation product of type III collagen (C3M) and type IV collagen alpha 3 chain known as tumstatin (TUM) (29,30). Numerous recent studies have confirmed the association of urinary C3M (uC3M) with renal fibrosis in different rat models including 5/6 Nx, anti-Thy 1.1, adenine nephropathy and type 2 diabetic nephropathy models (31,32).

DKD is associated with complex pathophysiological alterations, however, controlling blood glucose levels and blood pressure is the primary objective of DKD

treatment. Reducing intraglomerular pressure with angiotensin converting enzyme (ACE) inhibitors or angiotensin receptor blockers (ARB) remained the cornerstone of hypertension guidelines. Multiple large scale clinical trials have been investigating the protective effects of RAAS inhibitors (RAASi) in patients with normal-, micro-, or macroalbuminuria (33–37). It has been showed that RAASi treatment can prevent or delay the onset of microalbuminuria, lowers the risk for the development of overt proteinuria and reduce the rate of CKD progression. In addition, there are experiments suggesting that the renoprotective effects of these agents go beyond merely decreasing blood pressure (38–40). Animal experiments revealed that inhibition of RAAS ameliorates tubulointerstitial fibrosis, glomerular hypertrophy and mesangial matrix expansion in DKD (41–43). Although, these results indisputably underlie the exceptional role of these drugs in the therapy of diabetes associated renal consequences, the exact mechanisms are still unclear.

However, RAASi are not the only agents used for the treatment of diabetic patients which are proved to have remarkable renoprotective effect. At the beginning of 2000s sodium-glucose cotransporter 2 inhibitors (SGLT2i) have transformed the treatment of diabetic patients. Fundamentally, SGLT2i facilitate to lower blood glucose levels by blocking glucose reabsorption from the glomerular filtrate, however, it came to light that the majority of their beneficial mechanisms are independent of glycemic regulation (44). To date, it has been elucidated that these agents contribute to the mitigation of DKD by several pleiotropic effects including the reduction in inflammatory mediators, attenuation of renal hypoxia, and the amelioration of fibrosis (45–48). On the basis of growing evidence, indication of SGLT2i have become a key therapy in the management of CKD patients with and without DM.

1.1.3. Acute kidney injury

There is growing evidence that acute kidney injury (AKI) and CKD are in strong connection and likely promote each other (49–51). Contrary to prior theories, AKI results persistent deterioration of kidney function due to irreversible loss of kidney cells and nephrons. Initial nephron loss can be compensated by the hypertrophy of remaining one to maintain GFR. However, these conditions will eventually lead to further nephron loss (**Figure 2**), advancing the progression of CKD (52).

DOI:10.14753/SE.2023.2872

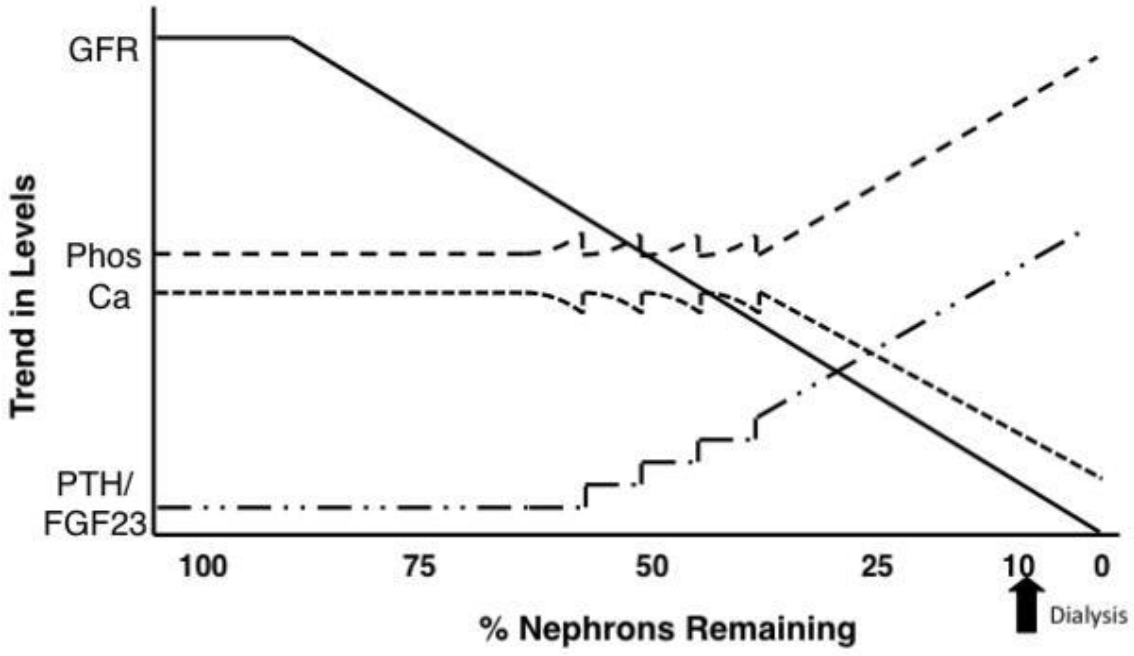

Figure 2. Levels of glomerular filtration rate (GFR), phosphorus (Phos), calcium (Ca) and parathyroid hormone (PTH) depending on the nephron number (53). Initial nephron loss can be compensated by nephron hypertrophy before the decline of GFR. Decreasing nephron number results the elevation of PTH to normalize unbalanced Phos and Ca levels.

There is a large variety of etiological factors of AKI. In high-income countries, AKI mainly endangers elderly patients with multiple comorbidities. In these settings, post-surgical interventions or other iatrogenic factors are the main causes (54). However, in low-income regions AKI occurs mostly as a complication of community-acquired causes such as sepsis, dehydration, toxins or pregnancy (55). The average pooled mortality rate is 23% in high-income countries, while in low-income countries this rate rises to 42%. Besides the more advance intensive hospitalization, this difference can be explained by the fact that in high-income countries 20-31.7% of the patients with AKI are already at in-hospital care (56).

Renal ischemia/reperfusion (IR) associated AKI is a common complication among hospitalized patients (incidence ~5%) which may significantly worsen the outcome of clinical interventions (57). Various pathophysiological factors can contribute to the manifestation of local or multi-organ ischemia including major surgeries, sepsis, traumatic dermal or blood loss and toxins (58). Renal IR injury is caused by a local impairment of oxygen and nutrient supply which leads to rapid changes in the metabolism

of kidney cells. In addition, due to its anatomical characteristics, outer medullary region is presumably vulnerable to hypoxic-ischemic insults. Renal countercurrent system is characterized by vasa recta, a capillary plexus located in the inner stripe of the outer medulla (**Figure 3)** (59). It facilitates the exchange of water and solute from the tubular fluid and the production of concentrated urine. However, vasa recta are extremely prone to vascular congestion caused by ischemia. In response to damaged endothelium, the expression of cell adhesion molecules increases, which induces the activation of leukocytes. Exaggeration of white blood cells results the obstruction of capillaries and the infiltration of the leukocytes into the renal interstitium. Interestingly, it has been shown that greater density of pericytes surrounding capillary vessels is associated with lower tubular damage and better outcome following renal IR (60).

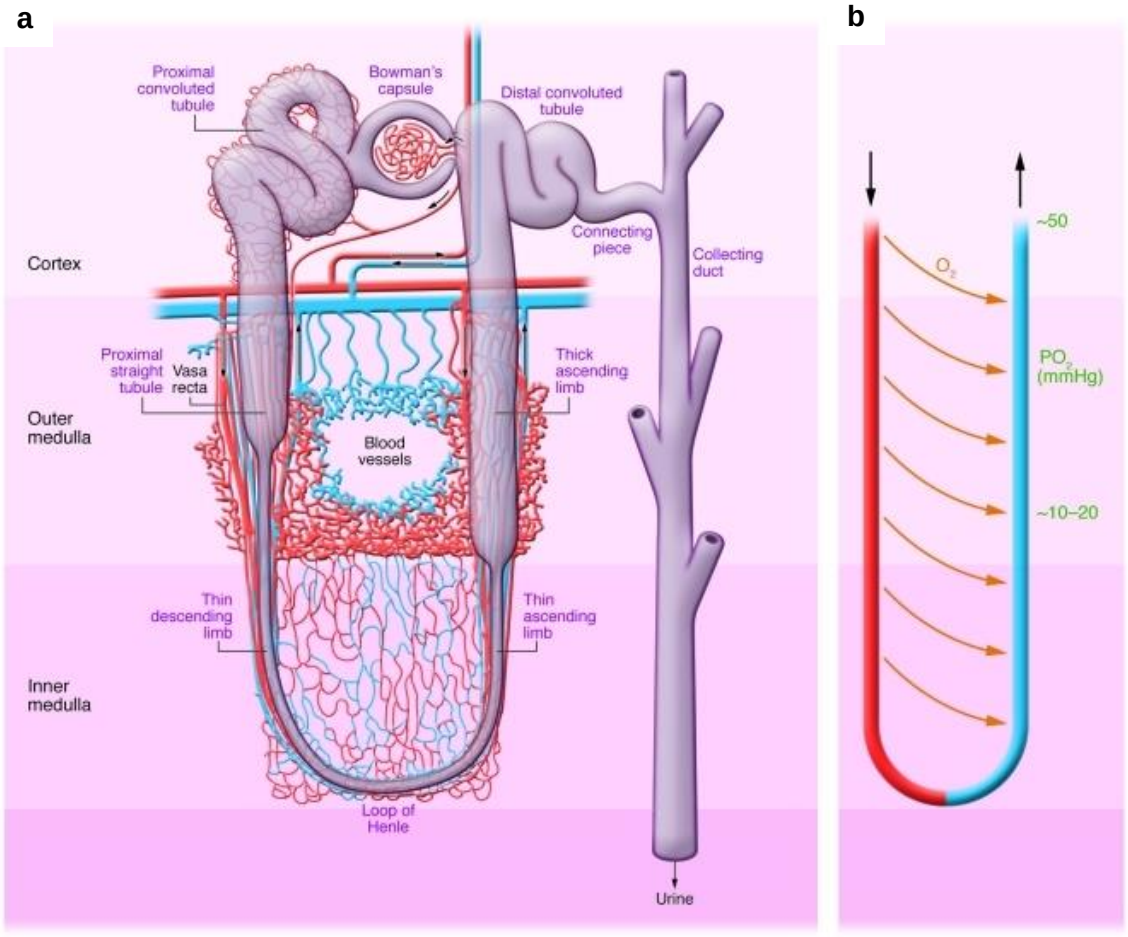

Figure 3. Nephron structure and the maintenance of the oxygen gradient (58). (a) Anatomy of nephron. Microvasculature of the outer medulla is peculiarly susceptible to hypoxic events. (b) The special capillary structure of vasa recta surrounding the descending and ascending limbs facilitates countercurrent exchange of oxygen resulting osmotic gradient between the blood and interstitial fluid.

Regardless of its origin, tubular damage and nephron loss are inevitably associated with AKI. Tubular necrosis is characterized by multiple stages including tubular lumen dilation, loss of brush border, vacuolization, eosinophilic hyaline casts of Tamm-Horsfall protein and eventually the presence of necrotic and/or apoptotic epithelial cells (61). Signs of epithelial cell injury caused by IR are the most plausible in the S3 segment of the proximal tubules.

In milder cases of IR, endogenous surviving tubular cells are able to replenish the tubular epithelium by dedifferentiation and proliferation. However, tubular damage usually results abnormal repair. Persistent tubulointerstitial inflammation, together with the hypoxic milieu promote the release of profibrotic cytokines such as TGF-ß and connective tissue growth factor (CTGF). This induces the transition of the renal epithelial and endothelial cells into myofibroblasts and initiating tubulointerstitial fibrosis.

The development of kidney fibrosis is facilitated by a complex interaction between various cell lineages within the injured area. Myofibroblasts play key role in the disease progression by producing ECM components such as collagen and fibronectin (62). In physiological condition, the abundance of myofibroblasts is low, however, their number increases greatly in the fibrotic tissue. Although, a broad range of cell types may be potential precursors of myofibroblasts (tubular epithelial cells, fibroblasts, pericytes, mesenchymal stem cells), their origin is still not completely elucidated (63–66). Following the injury, infiltrated immune cells and tubular epithelial cells secrete growth factors and other signal molecules like Wnt and Tissue Metallopeptidase Inhibitor 1 which facilitate myofibroblast activation via the initiation of proliferation and differentiation of progenitor cells (67). Alpha smooth muscle actin (α-SMA) is another key mediator of fibroblast activation, which is also expressed by pericytes and vascular smooth-muscle cells.

Regardless of the origins, tubulointerstitial fibrosis is the most consequent manifestation of CKD, thus the degree of fibrosis is the best indicator for the progression of the disease. *In vivo* studies on CKD animal models implicate different histological and molecular biological methods to measure the extent of fibrosis. However, suitable sample preparation, due to the focal nature of fibrosis, is still challenging.

DOI:10.14753/SE.2023.2872

1.2. Lyophilization

The practical applicability of freeze-drying, or lyophilization was first shown during World War II, implemented to provide human plasma on battlefields (68). A few years later, the technology has undergone a huge development, and became mainstream in the preservation of antibiotics and other liable pharmaceutical and biological products. Today, lyophilization is a cost-effective water removal method which is widely used in in the food- and pharmaceutical and biotechnological industry, and the technology is under steady expansion. Originally, it was developed to improve storage stability and to provide easier shipping, however, the area has numerous unexploited opportunities.

1.2.1. Principles of lyophilization

The process of lyophilization includes three main steps: pre-freezing, primary drying and secondary drying **(Figure 4)**. The key driving force of freeze-drying is sublimation, which facilitates the elimination of the solvent (typically water) from the sample under vacuum. Since catalytic enzymes remain in a solid environment throughout the whole process, it also preserves highly degradable molecules such as proteins and RNAs. However, lyophilization is a sensitive technique, which requires balanced working parameters determined by sample properties.

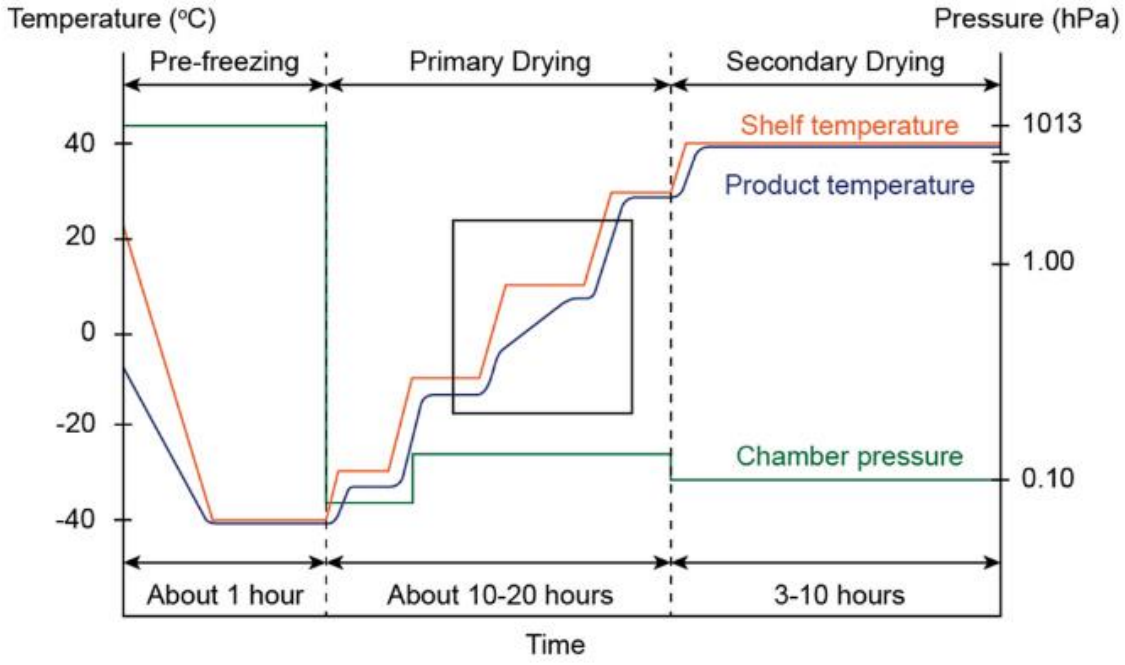

Figure 4. Main stages of freeze-drying. After the sample is perfectly frozen, shelf temperature is gradually raised, making sure that the product temperature does not reach the eutectic temperature specific for the actual composition. Temporary slow-down of product temperature increment (area with black frame) represents sublimation in the immediate environment of the Pt100 thermocouple sensor. Ideally, all of the free water is sublimed by the end of the primary drying step (10-20 hours). Finally, lower pressure and higher temperature is applied in the secondary drying phase to remove bound water (3-10 hours).

During pre-freezing, protein stability may be impaired by denaturation events including supercooling, freezeconcentration or crystallization, thereby, selecting the appropriate freezing process is critical (69). After the sample became completely frozen, vacuum is applied and the frozen water starts subliming by gradually increased temperature. Once this step is complete, temperature is further increased, resulting the removal of bound water molecules. This phase is called secondary drying.

The main challenge during primary drying is to avoid sample microstructure destruction, or so called “cake collapse”, which leads to the blockage of pores left by previously sublimed ice, thus the inhibition of complete drying. Cake collapse occurs, when the product temperature exceeds a critical temperature, which is determined by the actual solvent content and sample properties (70,71). Eutectic temperature (T_e) is a well-defined attribute of crystalline systems, where the substance changes state from solid to liquid. However, most freeze-drying samples contain amorphous phases, which are characterized by the glass transition temperature (T_g). Glass transition is a gradual transition of amorphous or semi-crystalline materials from solid state to a softer, deformable phase (**Figure 5)**. The collapse temperature (T_c) is a critical parameter of the freeze-drying process, which is close to the T_g of the maximally freeze concentrated solute. At this temperature, the material can no longer support its own structure and cake collapse occurs.

DOI:10.14753/SE.2023.2872

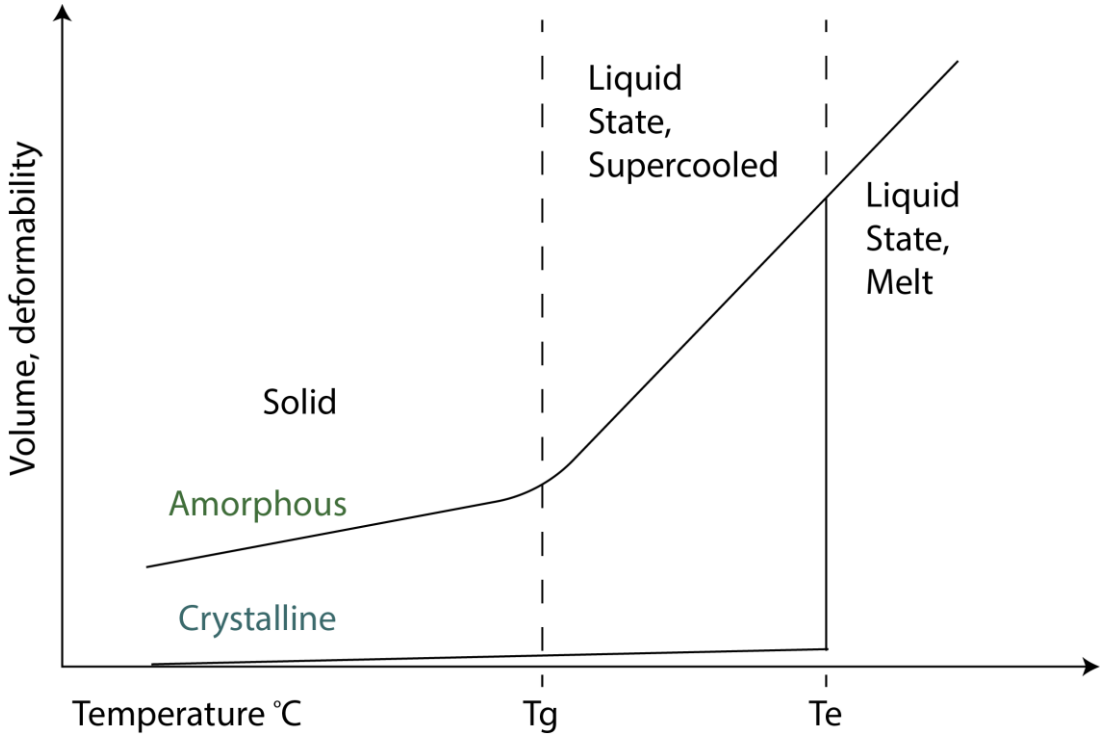

Figure 5. Phase transition of amorphous and crystalline materials. Amorphous substances are characterized with glass transition temperature (Tg) above which the material transform from solid state to a deformable, rubber-like phase. The eutectic temperature (Te) is a well-defined temperature, where the melting of crystalline matter occurs.

Generally, using slower heating ramp rates is a good way to maintain the product temperature below the T_c, however, time is a key limiting factor in case of industrial applications. Thereby, optimization of drying cycle is crucial to increase manufacturing throughput and to preserve sample quality **(Figure 6)**.

AIM	CONSIDERATIONS	OBJECT PROPERTIES	PARAMETERS TO ADJUST
Perfect drying	Collapse avoidance	• fraction of amorphous components → glass-transition temperature	• freezing temperature • ramp of drying
		• surface area • structure → drying rate	• ramp of drying
	Enough time for drying	• volume → water content	• time of drying
		• structure → drying rate	
Intact product structure	Size of ice crystals		• freezing rate

OPTIMIZATION OF LYOPHILIZATION

Figure 6. Main considerations during freeze-drying cycle optimization. Convenient drying and the preservation of desired sample properties such as structure or bioactivity are the key objectives of lyophilization. Generally, sample collapse can be avoided by keeping the product temperature below collapse temperature (~glass transition temperature) by regulating drying ramp. The length of drying is determined by various properties including sample volume, drying surface area, water content, composition and structure. Sample structure is also influenced by the size of the ice crystals thus, freezing rate can also be a critical factor.

Cycle optimization was first developed by trial and error approach which exclusively relies on empirical data. This means that a large number of experiments are performed with different values of shelf temperature and chamber pressure until the desired product quality attributes are achieved. However, this method is time consuming and most of the times, the estimated parameters does not match with the ideal setup.

Process analytical technology (PAT) is a system defined by the US Food and Drug Administration (FDA) which implement a range of tools such as quality by design (QbD) to improve process monitoring, scaling and controlling manufacturing (72). Modelling is an essential element of QbD to define Design Space and to reduce experimental workload (73,74). There are various thermoanalytical methods for determining Critical Process Parameters (CPP) like glass transition and collapse temperature, or primary drying endpoint, however, these require costly instruments and advanced expertise (75,76).

There are simpler devices such as thermocouples, which are one of the most popular tools for monitoring product temperature during lyophilization (77). These point sensors are easy to use due to their flexible and narrow design, however, simplicity entails a few limitations. Thermocouples, by their nature, are only able to detect product temperature at the point where the wires form a junction, thus, accuracy of this method may be suboptimal for defining drying endpoint. Therefore, additional experiments are needed to determine residual water content.

1.2.2. Lyophilization of biological samples

Freeze-drying of biopharmaceutical products and tissues are commonly used to increase storage stability, while it also makes shipping cheaper and easier. Generally, harvested tissue samples are snap frozen and stored at ultralow temperature (-80°C) before further molecular biological investigations. However, low temperature storage capacity of laboratories is usually limited, in addition, long shipping times and unhandy

ice containers makes transportation inconvenient. Properly dried samples are proved to be storable at room temperature without the degradation of protein and RNA content, since nucleases and proteolytic enzymes are inactive in the absence of mobile environment (78). Lyophilization is also popularly used for the preservation of living cells such as microbes, sperm cells or stem cells (79–81). However, it is essential to maintain cell viability and proper biological activity, therefore, use of cryoprotective agents are required to minimize structural and functional damage caused by freezing or drying.

DOI:10.14753/SE.2023.2872

2. Objectives

The current gold-standard for diagnosing and following-up the development of renal fibrosis is renal pathological biopsy due to the lack of sensitive, non-invasive biomarkers. Diagnosis is even more difficult in DKD where renal biopsy is taken only very rarely in complex cases.

Therefore, first we aimed to test novel urinary biomarkers of kidney fibrosis in experimental DKD rat model. Our results indicated that the current sample preprocessing methods used for the investigation of tissue fibrosis are not precise enough due to the focal nature of ECM accumulation. Therefore, we aimed to introduce a novel way of sample preparation such as freeze-drying and powdering for various biological specimens to achieve higher reproducibility. Furthermore, this work was also addressed to investigate and to validate the applicability of lyophilization as an alternative biological sample processing method.

The following objectives have been set to fulfill the aims:

1. To test novel urinary biomarkers of kidney fibrosis in DKD rat model.
2. To evaluate the anti-fibrotic effect of RAASi in DKD rat model.
3. To set up freeze-drying protocol for the rat kidney and other specimen (rat heart, lungs; human feces, peritoneal dialysis (PD) effluent).
4. To investigate the precision and long-term stability of protein and RNA level measurements in tissues preprocessed by lyophilization and/or pulverization.
5. To test the applicability of lyophilization for sample preprocessing of human feces and PD effluent.

DOI:10.14753/SE.2023.2872

3. Materials and Methods

Animal experimental protocol

Animal experiments were carried out in accordance with guidelines of the Council on Animal Care of the National Health Institution of Hungary (PEI/001/380-4/2013, PEI/001/1731-9-2015).

Clinical studies were approved by the Semmelweis University Regional and Institutional Committee of Science and Research Ethics (31224-5/2017/EKU, 19048-Á2/2018/EKU).

DM rat model:

Six-week old male Wistar rats (Rattus norvegicus, RGD Cat# 13508588, RRID:RGD_13508588; Toxi-Coop, Toxicological Research Centre; Dunakeszi, Hungary) were kept in temperature controlled room (24 ± 0.2 °C) under 12-hour dark/light cycle. Standard laboratory food and tap water was available *ad libitum*. Single intraperitoneal injection of 65 mg $bwkg^{-1}$ streptozotocin (STZ) in 0.1 M citrate buffer (pH 4.5) was used for DM induction. Diabetic rats were selected based on repeated blood glucose level measurement from the tail vein using a D-Cont IDEAL instrument (77 Elektronika, Budapest, Hungary). Rats with ≥15 mmol/L blood glucose concentrations were considered diabetic. Five weeks after the STZ induction rats were assigned into the following randomized groups (n=7-8/group) and were treated by oral gavage daily for 2 weeks: (i) isotonic saline as vehicle (D); (ii) Ramipril 10 µg $bwkg^{-1}$ (D + Ramipril); Losartan 20 mg $bwkg^{-1}$ (D + Losartan); Spironolactone 50 mg $bwkg^{-1}$ (D + Spironolactone); Eplerenone 50 mg $bwkg^{-1}$ (D + Eplerenone). Non-diabetic, age-matched animals (Control; n=8/group) served as controls. Control rats were treated with one-time intraperitoneal citrate buffer injection followed by daily oral gavage of saline, at the same time as the diabetic animals during the 2-week treatment period. After 2 weeks, rats were anaesthetised by a mixture of 75 mg $bwkg^{-1}$ Ketamine (Richter Gedeon, Budapest, Hungary) and 10 mg $bwkg^{-1}$ Xylazine (Medicus Partner, Biatorbagy, Hungary) followed by body weight measurement and terminal blood drawn. Blood, urine and kidney samples were collected and stored for further processing. Renal (blood urea nitrogen (BUN),

creatinine) parameters were determined using Hitachi 912 chemistry analyser (Roche Hitachi, Basel, Switzerland). Creatinine clearance were calculated.

Renal IR injury rat model:

8-week-old male Wistar rats (Toxi-Coop Toxicological Research Center, Dunakeszi, Hungary) were kept in standard laboratory cages. Rats had access to food and water *ad libitum*. Experiment were approved by the Committee on the Care of Laboratory Animals at Semmelweis University (Budapest, Hungary).

General anesthesia was induced by intraperitoneal injection of ketamine (75 mg/bwkg) and xylazine (10 mg/bwkg) mixture. Abdomen was opened and artery and vein of the left kidney were dissected and clamped for 50 minutes with atraumatic vascular clamp. The right kidney was removed before the reperfusion. After the clip was removed, kidney was observed for 5 minutes to visually confirm decent reperfusion. Kidney samples were collected 24 hours after the reperfusion. Kidney tissue samples were immediately frozen or fixed in buffered 4% formalin for further processing.

Human sample collection

Human peritoneal dialysis (PD) effluent samples were collected from children treated with PD at the Pediatric Center, Semmelweis University. Dialysis of patients was performed with PD solution containing 1.5% glucose (Fresenius Medical Care, Bad Homburg v.d. Höhe, Germany). Samples were collected in the morning after the first overnight home dialysis. Collected PD specimens were immediately frozen and stored at -80°C until further use.

Fecal samples were collected from healthy, inflammatory bowel disease and irritable bowel syndrome patients at the Pediatric Center, Semmelweis University. Samples were stored at +4°C for 24 hours, then aliquoted and stored at -80°C until further processing.

Biomarkers of ECM turnover

Levels of urinary Collagen type III breakdown product (uC3M), N-terminal pro-peptide of rodent type III collagen (rPRO-C3) and tumstatin (TUM) were measured using

competitive enzyme-linked immunosorbent assay (ELISA) kits developed by Nordic Bioscience (Herlev, Denmark). Urinary output levels were normalized to urinary creatinine levels determined with QuantiChromTM Creatinine kit (BioAssay Systems). Measurements were accomplished at the laboratory of Nordic Bioscience (Herlev, Denmark) according to previously described protocols (Genovese et al., 2016, Nielsen et al., 2018). Wells of streptavidin-precoated 96-well ELISA plates (Roche, cat. 11940279) were filled with 100 µL biotinylated peptide and incubated for 30 min at 20 ºC. Following repeated washing steps (x5) performed with washing buffer, 20 µL of standard peptide or a mixture of sample and HRP–conjugated monoclonal antibody were added to the wells and incubated for 20 h at 4 ºC (uC3M, rPRO-C3) or 1 h at 20 ºC (TUM). After 5 repeated washing steps, 100 µL of 3,3',5,5-tetramethylbenzidine (Kem-En-Tec, cat. 4380H, Taastrup, Denmark) were added to the wells and incubated for 15 min at 20 ºC in dark. Reaction was stopped by the addition of 1% sulfuric acid solution, and density values were measured with ELISA Microplate Reader (VersaMax, Molecular Devices, CA, USA) at 450 nm and 650 nm.

Extraction for metabolome analysis

Human fecal samples were prepared for metabolomics analysis by MxP® Quant 500 kit of Bioctares (Innsbruck, Austria) according to the Application Note 35035 (Heischmann 2018). A custom extraction was performed as following to test the applicability and efficiency of lyophilization. Two portions of 20-60 mg wet feces were processed and lyophilized. Dried sample mass was subsequently measured and recorded. The first fraction was extracted using ethanol:20 mmol/L phosphate buffer (pH=7.5) 85:15 (v/v), while extraction of the second fraction was performed using a 15:85 (v/v) composition of the same liquids. 500 µL extraction mixture was added to the dry sample with the container kept in an ice bath and was shaken on an orbital shaker at 200 rpm for 30 min. The procedure was repeated twice, and the products were combined for further analysis.

Lyophilization and product processing

Lyophilization and protocol setup was performed with a ScanVac CoolSafe Touch Superior device (LaboGene A/S, Allerod, Denmark). Harvested rat tissue samples were

divided in small (~20 mm^3) pieces, arranged in 2 mL plastic tubes to attain the largest surface and stored at -80°C until freeze-drying **(Figure 7a)**. Tubes remained open during the entire freeze-drying process **(Figure 7b)**. Sample temperature was monitored using a Pt 100 thermocouple placed in the core of a chosen piece of tissue **(Figure 7c)**. Dried products were manually shattered with needles (20 Gauge) and powdered with 5 mm stainless steel beads using a TissueLyser LT (Qiagen GmbH, Hilden, Germany) instrument. To maximize drying surface, PD effluent was snap-frozen on the wall of a 50 mL plastic tube in liquid nitrogen **(Figure 7d)**. Powdered tissue samples were stored at 4°C. Residual water content of lyophilized tissues was determined using the classic Karl Fischer titration (82).

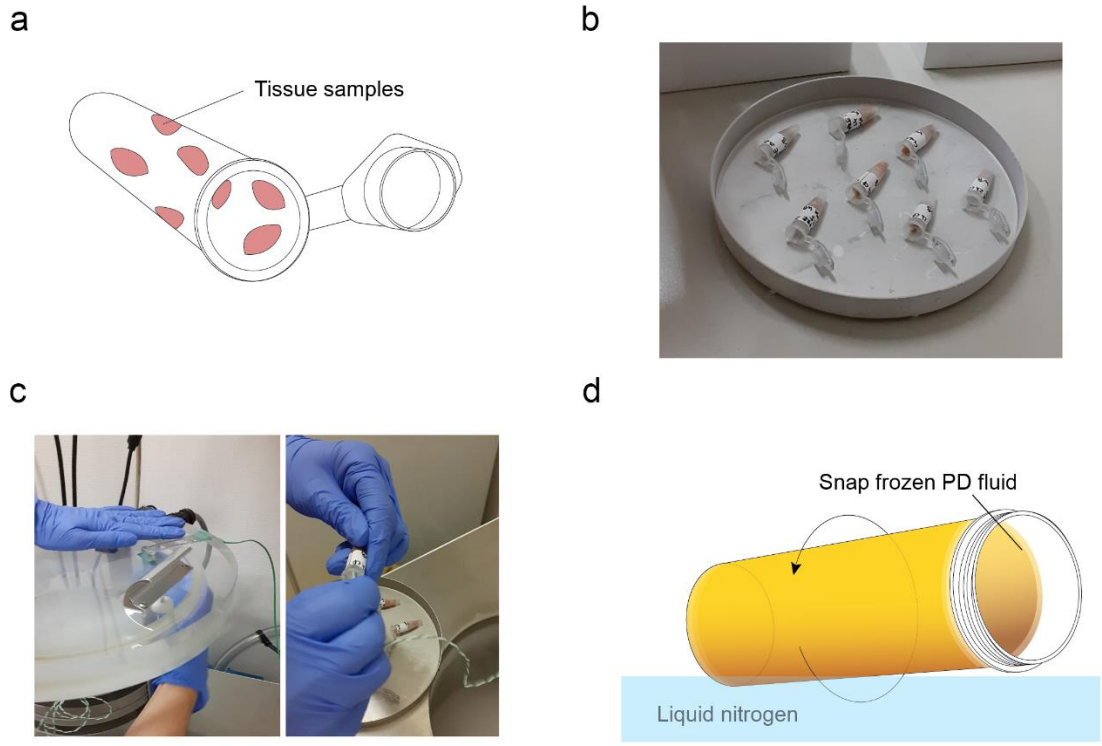

Figure 7. Sample preparation for freeze-drying. (a) Tissue samples should be cut in pieces and optimally arranged in the container to achieve high surface-area-to-volume ratio. (b) Tubes are kept open throughout the entire process. Make sure that drying is not obstructed by other samples. (c) Thermocouple sensors should be placed in the core of the sample to monitor product temperature. (d) Snap freezing to the wall of the container by spinning in liquid nitrogen is recommended in case of liquid samples to optimize drying surface.

Reverse transcription quantitative polymerase chain reaction (RT-qPCR)

Total RNA isolation Mini Kit (Geneaid Biotech, New Taipei City, Taiwan) was used to extract total RNA from rat kidney and heart tissues according to the manufacturer's instructions. Quality and quantity of isolated RNA were measured with NanoDrop ND-1000 spectrophotometer (BCM, Huston, TX, USA). First strand cDNA was revers transcribed using Maxima First Strand cDNA Synthesis Kit for RT-qPCR (Thermo Fisher Scientific, Waltham, MA, USA). Relative gene expression was determined by RT-qPCR using 1 μL cDNA samples, 10 μL SYBR Green I Master enzyme mix (Roche Diagnostics, Mannheim, Germany) and 10 pmol μL^{-1} of each specific primer (IDT, Coralville, Iowa, USA (primer sequences: Table 1). Qualitative and quantitative analysis were performed by LightCycler 96 software version 1.1.0.1320 (Roche Diagnostics, Mannheim, Germany).

Table 1. RT-PCR primer sequences used in this study (GAPDH: Glyceraldehyde 3-phosphate dehydrogenase, NGAL: Neutrophil gelatinase-associated lipocalin; T_a: annealing temperature)

Gene name	Regular name	NCBI ID	Primer pairs		Product length	T_a
Gapdh	rat GAPDH	NM_017008.4	Forward:	5'-CAC CAC CAT GGA GAA GGC TG-3'	240 bp	60°C
			Reverse:	5'-GTG ATG GCA TGG ACT GTG-3'		
Acta2	rat alpha smooth muscle actin	NM_031004.2	Forward:	5'-GAG CGT GGC TAT TCC TTC GTG-3'	106 bp	60°C
			Reverse:	5'-CAG TGG CCA TCT CAT TTT CAA AGT-3'		
Rn18s	rat 18S ribosomal RNA	NR_046237.1	Forward:	5'-GCG GTC GGC GTC CCC CAA CTT CTT-3'	105 bp	60°C
			Reverse:	5'-GCG CGT GCA GCC CCG GAC ATC TA-3'		
Havcr1	rat kidney injury molecule 1	NM_173149.2	Forward:	5'-CGC AGA GAA ACC CGA CTA AG-3'	194 bp	60°C
			Reverse:	5'-CAA AGC TCA GAG AGC CCA TC-3'		
Lcn2	rat NGAL	NM_130741.1	Forward:	5'-GGG CTG TCC GAT GAA CTG AA-3'	98 bp	60°C
			Reverse:	5'-CAT TGG TCG GTG GGA ACA GA-3'		

Western blot analysis

Frozen and lyophilized samples were suspended in protein lysis buffer (1 M Tris, 0.5 M EGTA, 1% Triton X-100, 0.25 M NaF, 0.5 M phenylmethylsulfonyl fluoride, 0.5 M sodium orthovanadate, 5 mg x mL^{-1} leupeptin, and 1.7 mg x mL^{-1} aprotinin, pH 7.4). Lysates were centrifuged at 13,000 rpm, 4°C for 10 min. Protein concentration of the supernatant was measured by Detergent Compatible Protein Assay Kit (Bio-Rad Hungary, Budapest, Hungary). Protein samples were denatured and separated on 4-20% gradient Mini-PROTEAN TGX SDS-polyacrylamide precast gel (Bio-Rad Hungary, Budapest, Hungary). PD effluent was rehydrated and used as total protein solution without denaturation. Total protein was transferred to nitrocellulose membranes. Membranes were blocked in non-fat milk buffer for 1 hour at room temperature and incubated in specific primary antibody solution overnight at 4°C, followed by horseradish peroxidase-conjugated secondary antibody solution (Cell Signaling Technology, Leiden, Netherlands) (Table 2). Signal detection was obtained with Molecular Imager VersaDoc MP 4000 System (Bio-Rad Laboratories, Hercules, CA, USA) using Luminata Forte (Millipore Corporation, Billerica, MA, USA) substrate. Quantity One Analysis 4.6.6 software was used for densitometric analysis of bands of interest (Bio-Rad Laboratories, Hercules, CA, USA). Results were normalized for Ponceau S staining and intermembrane control.

Table 2. List of antibodies used for Western blot (αSMA: alpha smooth muscle actin; pAkt: phospho-protein-kinase B; peNOS: phosphorylated endothelial nitric-oxide synthase, CTGF: connective tissue growth factor)

Antibody	Vendor	Catalogue number	Dilution	Secondary antibody	Secondary antibody dilution	Secondary incubation time
αSMA	Sigma-Aldrich, Darmstadt, Germany	A2547	1:500	goat anti-mouse IgG	1:6000	30 minutes
pAkt	Cell Signaling Technology, Leiden, Netherlands	4060S	1:1000	goat anti-rabbit IgG	1:4000	30 minutes
Akt	Cell Signaling Technology, Leiden, Netherlands	9272S	1:1000	goat anti-rabbit IgG	1:3000	1 hour

peNOS	Cell Signaling Technology, Leiden, Netherlands	9571S	1:1000	goat anti-rabbit IgG	1:3000	1 hour
eNOS	Abcam, Cambridge, UK	66127	1:1000	goat anti-rabbit IgG	1:5000	1 hour
CTGF	Santa Cruz Biotechnology, Dallas, USA	sc-14939	1:1000	rabbit anti-goat IgG	1:5000	1 hour

Renal histology

Rat kidney tissues were fixed in 4% neutral buffered formaldehyde, dehydrated in graded alcohol series, embedded in paraffin, cut to 3 μm thick sections and mounted on coated glass microscope slides. Sections were stained with, periodic acid-Schiff (PAS) Masson's trichome or Picrosirius red reagent. Fibrotic interstitial areas were visualized on 10-200x magnification with Panoramic Viewer software version 1.15.2 (3DHISTECH, Budapest, Hungary). Quantitative analysis was performed with Adobe Photoshop 2016 (San José, California, USA) and ImageJ (U. S. National Institutes of Health, Bethesda, Maryland, USA).

Terminal deoxynucleotidyl transferase dUTP nick end labeling (TUNEL) assay

Formalin-fixed rat kidney samples were embedded into paraffin. Sections of 5μm were cut and mounted on Superfrost slides (Thermo Shandon, Runcorn, UK) followed by manual removal of the paraffin. Preprocessing and labelling of apoptotic cells were performed by TUNEL assay using Apoptag® Peroxidase In situ Apoptosis Detection Kit (Millipore, Billerica, MA, USA). Samples were incubated in Proteinase K for 15 min and washed before blocking endogenous peroxidase activity with 3% H2O2:methanol mixture. Sections were incubated in reaction buffer containing 30% TdT enzyme for 1 hour at room temperature after which Stop buffer was added. Slides were incubated with anti-Dioxigenin Conjugate for 30 min at room temperature. Color reaction was catalyzed using DAB peroxidase substrate. Slides were digitalized with Mirax scanner and images were taken with CaseViewer 2.4 software (3DHISTECH Ltd.).

Immunohistochemistry

Rat kidney tissues were fixed in formalin, embedded into paraffin and 5μm sections were cut. Samples were placed in 1mM (pH=6.0) citrate buffer and heated in a microwave oven for 15 minutes to induce epitope retrieval. Following cooling, samples were washed in TRIS buffered saline (TBS; pH=7.6) and incubated in anti-CD45 antibody (Cat. Nr. ab10558, Abcam plc., 1:500) for 1 hour at room temperature. After repeated washing steps, sections were incubated in HISTOLS-R anti- rabbit HRP labelled detection system (Cat. Nr. 30011.R500, Histopathology, Ltd.) for 30 minutes at room temperature. Samples were washed with TBS and reaction was developed with HISTOLS Resistant AEC Chromogen/substrate System (Cat. Nr. 30015.K, Histopathology, Ltd.) controlled under light microscope. Hematoxylin eosin solution was used to counterstain sections, following bluing with tap water. Sample dehydration was performed with alcohol. Sections were purified in xylene and mounted with permanent mounting medium. Slides were digitalized with Mirax scanner and images were taken with CaseViewer 2.4 software (3DHISTECH Ltd.).

Immunofluorescence

Following the embedding in Shandon cryomatrix (Thermo Fisher Scientific, Waltham, MA, USA) frozen rat kidney samples were cut into 10 μm sections. Slides were incubated in anti-αSMA primary antibody (Sigma-Aldrich, Cat. No. A2547, RRID:AB_476701; dilution=1:1000) for 2 hours. After repeated washing steps, anti-mouse IgG Alexa fluor 488 secondary antibody (Thermo Fisher Scientific, Cat. No. A-11001, RRID:AB_2534069; dilution=1:100) was added and slides were incubated for 1 hour at room temperature. Nuclei was visualized with Hoechst 33342 (Cell Signaling Technology, Cat. No. 4082S, RRID:AB_10626776; dilution=1:1000). Samples were fixed with Vectashield Mounting Medium (Vector Laboratories, Cat. No. H-1000, RRID:AB_2336789). Analysis was performed using Zeiss LSM 510 Meta confocal laser scanning microscope (LSM Image Examiner, RRID:SCR_014344) with 63× or 100× magnification objectives.

Statistical analysis

Statistical analyses were performed using GraphPad Prism software version 7 (GraphPad Software, San Diego, CA, USA). Sample distribution was determined by Kolmogorov-Smirnov normality test. The effects RAASi were tested by one-way ANOVA followed by Bonferroni's multiple-comparison post hoc test in case of normally distributed data and by Kruskal-Wallis in case of non-parametric data. The effects of lyophilization protein and RNA content were analyzed using two-tailed paired t-test for parametrical comparisons and Wilcoxon test in case of the failure of Kolmogorov-Smirnov test. Absolute differences were analyzed by Levene's test using Microsoft Office Excel (Microsoft, Redmond, WA, USA). *P* values of <0.05 were considered significant.

4. Results

Urinary markers of collagen turnover signify the development of kidney fibrosis

Our experiments revealed higher kidney to body weight ratio and declined kidney function following STZ induction which signifies the development of DKD **(Figure 8a)**. Kidney enlargement and increased blood urea nitrogen levels were reduced by all the investigated RAASi. Although, RAASi did not lower increased serum creatinine levels, Ramipril, Spironolactone and Eplerenone restored the declined creatinine clearance.

DM resulted increased urinary levels of rPRO-C3, uC3M and TUM indicating enhanced type III collagen formation, degradation, and type IV collagen turnover respectively **(Figure 8b)**. Levels of uC3M were decreased in Eplerenone treated rats.

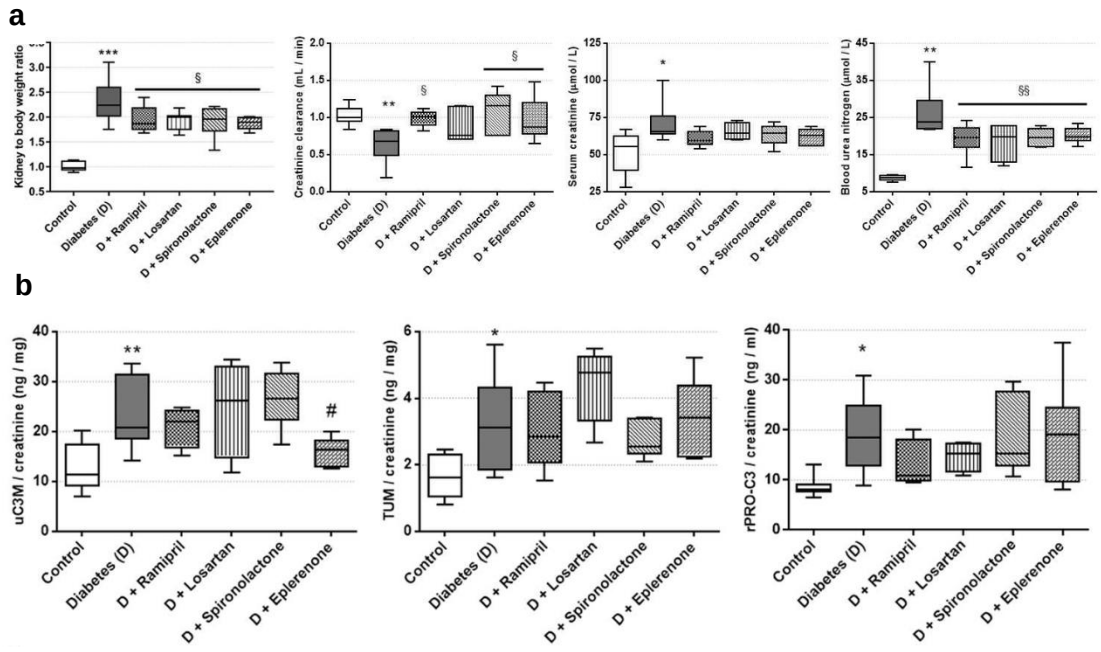

Figure 8. Renal function parameters and urinary markers of kidney fibrosis. (a) Renin-angiotensin-aldosterone system inhibitors (RAASi) improve renal parameters of diabetic rats. (b) Increased levels urinary type III collagen degradation fragment (uC3M), tumstatin (TUM) and N-terminal pro-peptide of rodent type III collagen indicates the development of renal fibrosis, but does not reflect the beneficial effects of RAASi treatment. Data are presented as means ± 95% confidence intervals. Analysis was performed with one-way ANOVA followed by Bonferroni′s multiple-comparison *post hoc* test; n = 7–8 rats/group; $^{*}P < 0.05$, $^{**}P < 0.01$, $^{***}P < 0.001$ *vs*. control; $^{\#}P = 0.08$, $^{\S}P < 0.05$, $^{\S\S}P < 0.01$ *vs*. D.

RAAS inhibitors reduce the extent of tubulointerstitial fibrosis in diabetic kidneys

We investigated fibrotic processes, including the accumulation of ECM components like collagen to estimate the manifestation of DKD. Renal tubulointerstitial fibrosis was assessed on Masson's trichrome-stained sections. The quantity of fibrotic connective tissue increased in diabetic animals, while all of the RAASi decreased tubulointerstitial fibrosis **(Figure 9a,b)**. To assess accumulation of the collagen components of the ECM, Picrosirius Red staining was performed, which showed increased amount of collagen in diabetic kidneys. RAASi also significantly decreased renal collagen depositions. Another widely accepted important and specific marker of fibrosis is the increased level of αSMA, indicating the activation and differentiation of fibroblasts. We demonstrated that in diabetic animals, the level of αSMA is significantly

increased and the protein is mainly localised in the tubulointerstitial region. RAASi decreased the accumulation of αSMA protein **(Figure 9c**).

DOI:10.14753/SE.2023.2872

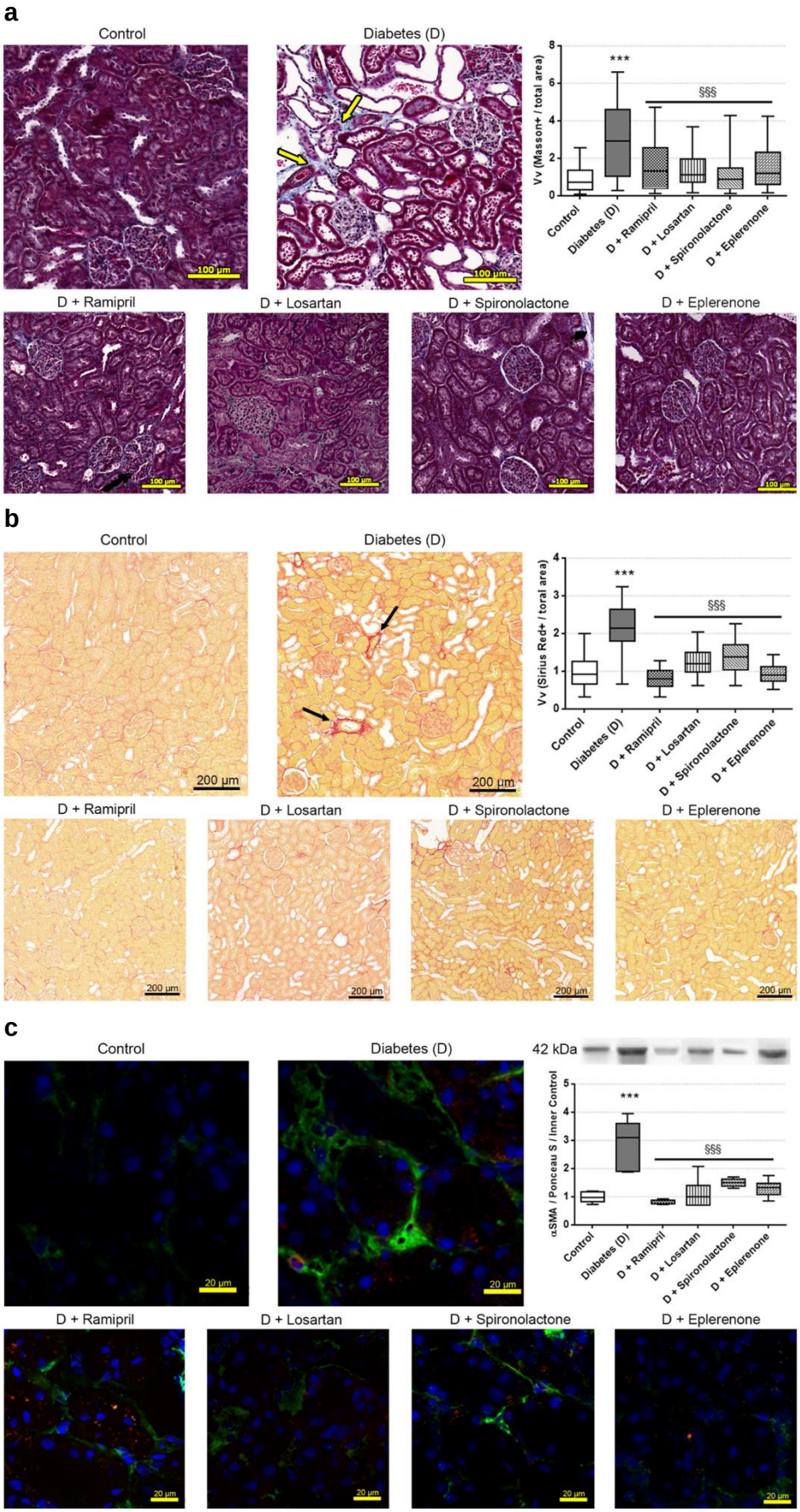

Figure 9. Detection of fibrosis in diabetic rat kidney. (a) Masson's trichrome (scalebar=100 μm) and (b) Picrosirius red (scalebar=200 μm) staining shows extracellular matrix component enrichment in diabetic rat kidneys, which is mitigated by the renin-angiotensin-aldosterone system inhibitor (RAASi) treatment. (c) Immunofluorescent histochemistry (scalebar=20 μm) and Western blot analysis demonstrates increased levels of renal αSMA, which is decreased by RAASi. Analysis was performed with one-way ANOVA followed by Bonferroni′s multiple-comparison *post hoc* test; n = 7–8 rats/group; $^{***}P < 0.001$ *vs.* control; $^{§§§}P < 0.001$ *vs.* D.

Freeze-drying protocol setup for rat kidney tissue

Precise determination of tissue injury and fibrosis proved to be challenging due to the inhomogeneous nature of structural damage and depletion of fibrotic chunks **(Figure 10a-d)**. Histological analysis and molecular biological investigations of tissue damage and fibrosis usually resulted highly dispersed data in former experiments **(Figure 10e)**. We hypothesized that an advanced way of sample preparation by freeze-drying and powdering would improve the precision of molecular biological measurements by creating more homogeneous sample pools. However, due to the lack of definitive process parameters in the literature regarding to biological specimens, first, freeze-drying protocols for various rat and mouse tissues were established.

Freeze-drying protocol was set up for rat kidney tissue based on the trial and error approach. Product temperature changes recorded by the Pt 100 thermocouple sensor confirmed the process of sublimation in the core of the tissue **(Figure 10f)**. Lyophilized kidneys showed no signs of wet spots, and they were proved to be properly dustable **(Figure 10g,h)**. Karl Fischer titration showed a mean residual moisture content of 1.5 ± 0.20 m/m% (n=5).

DOI:10.14753/SE.2023.2872

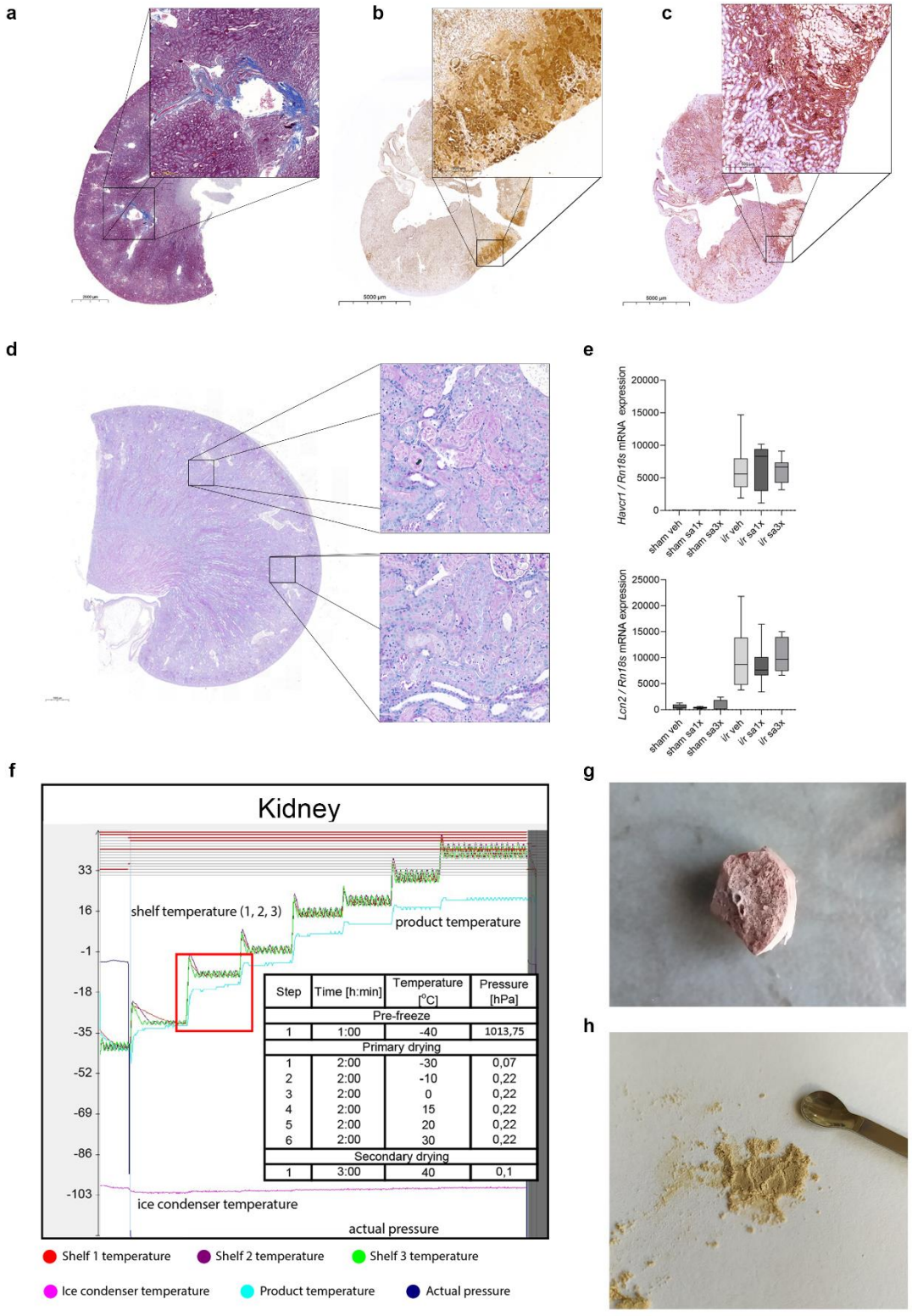

Figure 10. Setting up freeze-drying protocol for rat kidney tissue to improve the precision of focal damage evaluation. Representative images of (a) Masson's trichrome staining, (b) TUNEL assay, (c) CD45 labeling and (d) periodic acid-Schiff staining demonstrates the inhomogeneous development of (a) diabetic and (b-d) ischemic kidney injury. Focal kidney damage may bias the measurement of injury

associated biomarkers such as (e) Kidney injury molecule 1 (*Havcr1*) and neutrophil gelatinase associated lipocalin (*Lcn2*), resulting high dispersion. Results were analyzed and normalized to the expression of *Rn18s* housekeeping gene from the same samples as reference transcript. (f) Freeze-drying protocol was established for rat kidney tissue. Red frame indicates sublimation period in the immediate environment of the Pt 100 thermocouple. (g) The lyophilized product shows no sign of wet spots and (h) it is properly dustable.

Lyophilization followed by powdering improves the precision of the measurement of RNA and protein levels

To test whether lyophilization followed by homogenization as an alternative way of sample preparation improves the precision, first we compared αSMA protein levels in conventionally preprocessed (frozen) and lyophilized, total rat kidneys **(Figure 11a)**. Our results revealed a strong outlier in the frozen group indicating inhomogeneous protein distribution.

To confirm our findings, we established and experimental set as follows. Four replicates of total protein and RNA extraction were performed conventionally from 4 different segments of a halved diabetic rat kidney sample, and four replicates of extraction were performed from the other half of the same kidney following lyophilization and homogenization **(Figure 11b)**. mRNA expression of *Acta2* and protein levels of αSMA and showed significantly lower variance in the lyophilized, homogenized group compared to conventionally processed frozen samples **(Figure 11c,d)**.

DOI:10.14753/SE.2023.2872

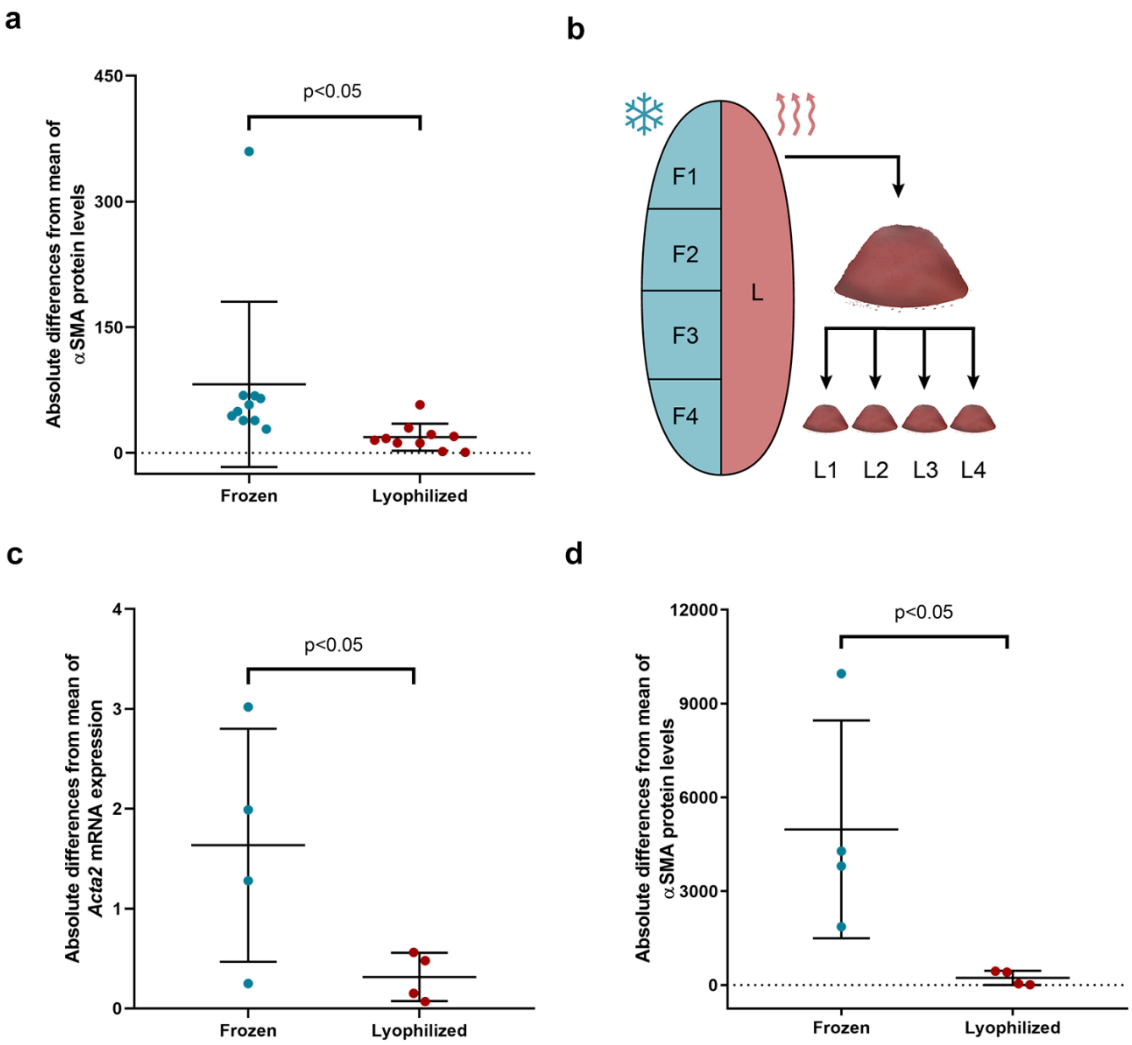

Figure 11. Comparison of the precision of protein and RNA measurements between kidney samples prepared conventionally and lyophilized. (a) Absolute differences from the mean of alpha smooth muscle actin protein (αSMA) levels are higher in conventionally preprocessed (frozen) diabetic rat kidneys compared lyophilized and powdered samples (n=10/group) (b) Schematic of sample preparation for comparative investigations. Diabetic rat kidney was divided in two and treated as follows: one half was lyophilized (L), powdered, and protein and RNA were isolated from four proportions of the homogenous powder (L1-L4); the other half was cut in four pieces frozen, and each fragment went through conventional protein and RNA isolation (F1-F4). Absolute differences from mean of (c) alpha smooth muscle actin gene (*Acta2*) expression and (d) αSMA protein levels are higher if protein and RNA isolation are performed from frozen segments *vs.* portions taken from lyophilized and powdered half of diabetic rat kidney (n=4 frozen and 4 powdered portions of the same kidney). Data were analyzed with Levene's test. Results were analyzed and normalized to the expression of *Rn18s* housekeeping gene from the same samples as reference transcript.

RNA and protein stability are preserved in lyophilized samples following long-term storage

We successfully applied the above-described freeze-drying protocol on other tissues, such as rat heart, and lungs **(Figure 12a)**. The residual moisture content was 0.47 ± 0.13 m/m% (n=5) in the heart and 3.02 ± 1.37 m/m% (n=5) in the lungs samples which both considered suitable. Due to the smaller absolute size, same protocols can be used in the case of mouse tissues (data not shown).

To investigate long-term storage stability of protein and RNA content, rat kidney and heart samples were processed as follows. Organs were divided in two, half of the tissues were stored frozen at -80°C, and the other halves were lyophilized and stored at 4°C for 20 months. RT-qPCR measurements revealed that levels of *Acta*2 and *Gapdh* mRNA did not change following lyophilization in comparison with tissues parts stored frozen **(Figure 12b,c)**. After the storage period we measured ubiquitously present proteins as well as their degradation-sensitive phosphorylated forms. Protein levels of αSMA, the ratio of phosphorylated Protein kinase B (pAkt)/ Protein kinase B (Akt) and the ratio of phosporylated endothelial nitric-oxide synthase (peNOS)/ endothelial nitric-oxide synthase (eNOS) did not decrease in rat kidney and heart samples during freeze-drying followed by long-term storage at 4°C **(Figure 12d-f)**. Moreover, in case of two samples phosphorylation remained more preserved in lyophilized samples compared to frozen ones.

DOI:10.14753/SE.2023.2872

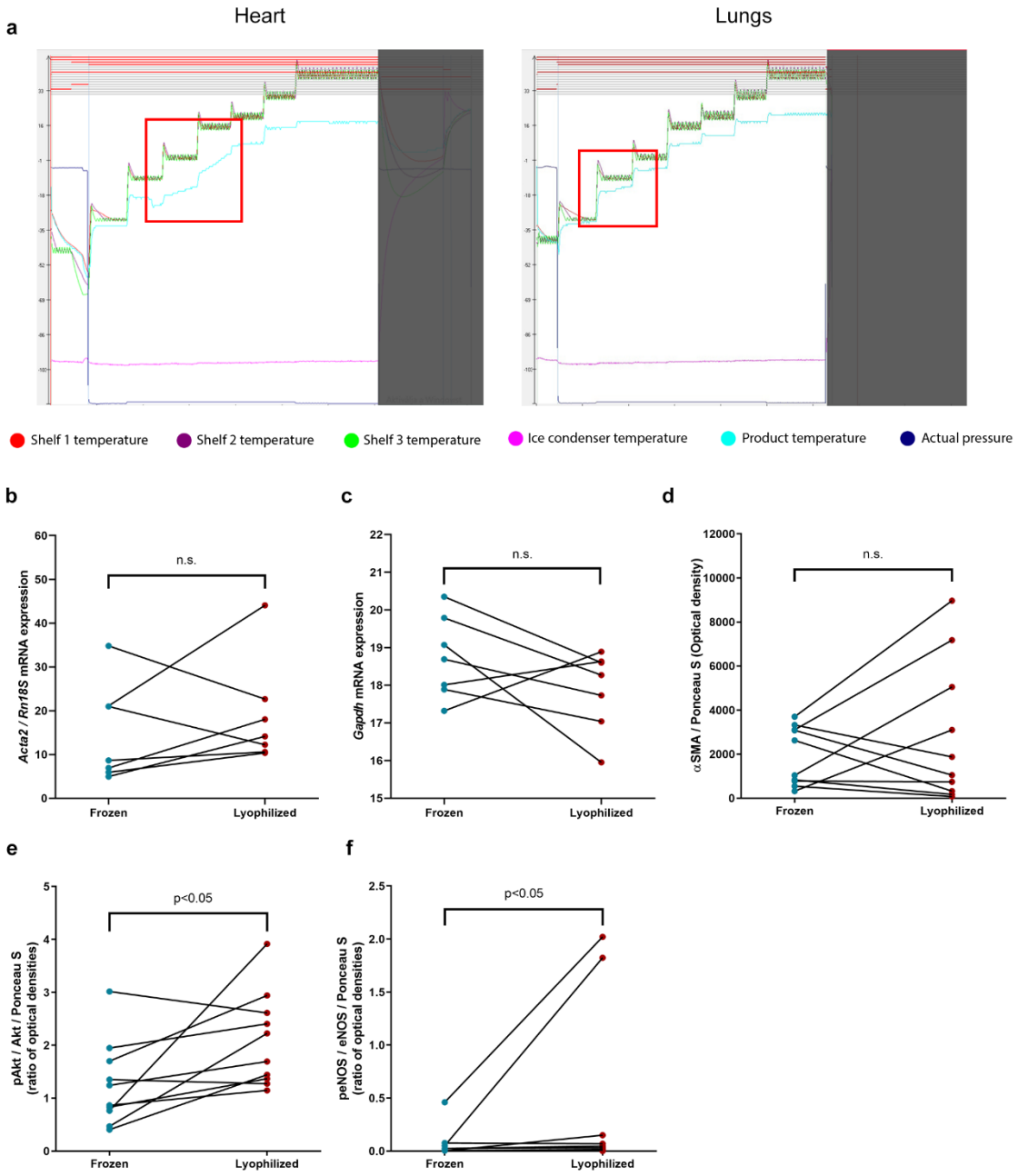

Figure 12. Long-term storage stability of protein and RNA content of frozen and lyophilized sample pairs of rat kidney and heart tissues. (a) Temperature and pressure characteristics of the freeze-drying process applied on rat heart and lung tissues. Red frames indicate sublimation period in the immediate environment of the Pt 100 thermocouple. To compare long-term storability, healthy rat kidney and heart sample pairs taken from the same tissue and stored either frozen at -80°C or lyophilized at 4°C for 20 months. Levels of (b) alpha smooth muscle actin mRNA (*Acta2*), (c) glyceraldehyde 3-phosphate dehydrogenase (*Gapdh*) mRNA, and (d) alpha smooth muscle actin protein (αSMA) remain equally preserved in frozen and lyophilized samples after long-term storage. (e) Phosphorylated protein-kinase B (pAkt)/Akt protein ratio and (f) phosphorylated endothelial nitric-oxide synthase (peNOS)/eNOS protein

ratio are higher in samples stored lyophilized compared to frozen ones. Data were analyzed with paired t-test (n=7 frozen-lyophilized sample pairs, n.s.=not significant).

Modified protocol is applicable for non-tissue type biological samples

Our experiments demonstrated that application of lyophilization in experimental research offers untapped opportunities. However, it can also be utilized in clinical studies as an improved way of human sample preprocessing. We established freeze-drying protocols for human PD effluent and feces to achieve a gentle way of sample preparation before further investigations. Primary drying time was modified to optimize the duration by increasing heating ramp and shortening the following phases **(Figure 13a,b)**.

By lyophilizing and rehydrating PD fluid we were be able to attain x20 concentration without the degradation of protein content. This kind of preprocessing gave us the chance to detect proteins with potential diagnostic value such as CTGF, which was inaccessible by Western blotting after conventional sample preparation **(Figure 13c)**.

Lyophilized fecal specimens have been used for metabolome analysis, which requires the removal of water before the quantitative investigation of components. Both absolute **(Figure 13d)** and relative **(Figure 13e)** amount of the detected substances of each classes were higher in lyophilized samples compared to those were preprocessed with MxP® Quant 500 KIT according to the manufacturer's instructions.

DOI:10.14753/SE.2023.2872

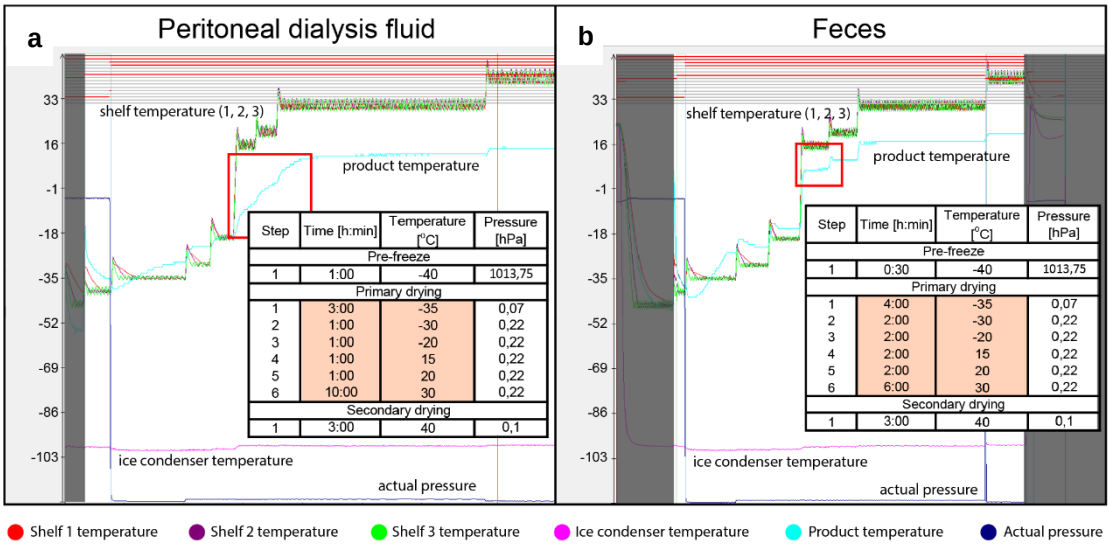

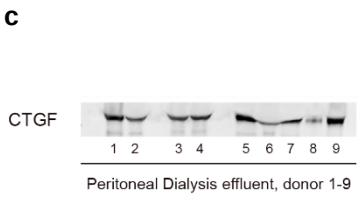

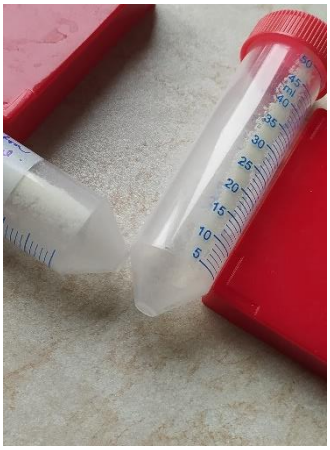

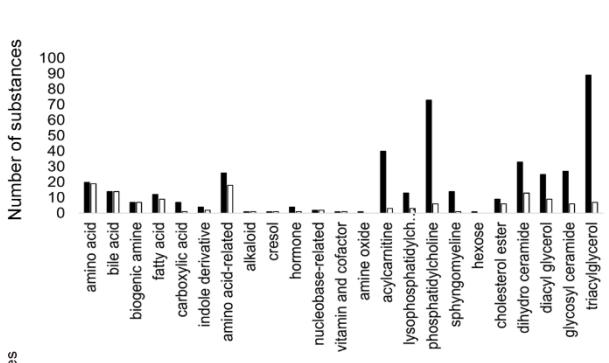

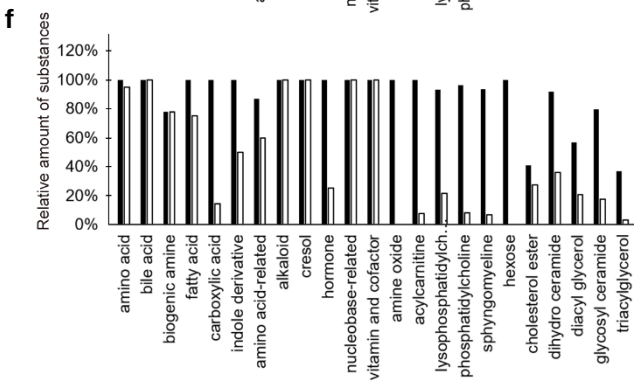

Figure 13. Application of freeze-drying on human peritoneal dialysis effluent (PDE) and feces. Lyophilization protocols and temperature and pressure characteristics of the freeze-drying process applied on human (a) PDE and (b) fecal specimens. (c) Concentration by lyophilization facilitates the detection of low abundance proteins such as connective tissue growth factor (CTGF) in PDE of nine human donors. (d) Representative image of the PDE following lyophilization. (e) The number and (f) the relative amount of substances (Y-axis) detected are higher in human fecal samples preprocessed with lyophilization (black bars) *vs.* with the commercially available kit (white bars).

5. Discussion

DKD is a frequent consequence of DM resulting serious complications and reduced lifespan, which creates an unsustainable strain on healthcare and society. RAASi and SGLT2i are the gold standard therapies, but even these compounds cannot reverse disease progression, thus early diagnosis and well-timed therapeutic intervention are desperately needed. Percutaneous kidney biopsy is the primary guideline for monitoring the manifestation of renal compromises, such as tubulointerstitial fibrosis, however, it is particularly performed on well-founded occasions due to its invasive nature and relative risk. Thereby, there is a great demand for both prognostic and endpoint biomarkers for routine clinical diagnosis. Here we tested novel urinary biomarkers of the ECM turnover, which may be promising indicators of renal fibrosis.

To date, urinary levels of collagen procession products have been associated with the development of kidney fibrosis induced by various chronic diseases such as lupus nephritis, IgA nephropathy and DM (83–86). Moreover, serum PRO-C3 showed independent correlation with mortality, suggesting that it may reflect a systemic condition. Here we confirmed the prognostic value of novel urinary biomarkers of collagen formation and degradation on diabetes induced kidney fibrosis. In addition, we proposed TUM, an endogenous antiangiogenic protein fragment of type IV collagen as a potential candidate of DKD and ESRD detection. Elevated urinary C3M, PRO-C3 and TUM implied the presence of kidney fibrosis, which was validated by our histological findings. Although, RAASi treatment significantly improved renal function and reduced the extent of ECM deposition and fibroblast activation, these finding were not reflected by the urinary markers.

In line with previous results, present experiments revealed highly scattering data which may be ambiguous when interpreting of typically inhomogeneous tissue damage such as fibrosis and focal necrosis. Therefore, to tackle this problem we introduced freeze-drying as a sample preprocessing method of biological tissues to achieve higher precision in addition to well-known benefits such as improved storage- and shipping stability. Although, lyophilization is widely used for removing water from biological specimens, detailed public protocols are lacking (87–89). Thereby, we set up suitable freeze-drying parameters for various biological samples including the rat kidney; heart; lungs, human PD effluent and feces. There are several instrumental analytical methods used in the

industry to determine critical freeze-drying parameters such as T_g and drying end-point, which is crucial for cycle optimization and thus, for increasing yield (90–93). However, these methods require advanced expertise and high-priced instruments that are not part of standard research laboratory equipment. We used Pt 100 thermocouples for monitoring product temperature changes that indicate sublimation. The quality of drying was verified by visual properties such as product structure and dustability which are key factors while pursuing homogeneous samples. The residual water content of rat kidney, heart, and lung tissues after secondary drying was below 3.5% which is considered appropriate in biological samples (87).

Previous results of ours and other groups have showed that conventional sample preprocessing methods might lead to inconsistent data and outlier values in case of biochemical investigations of focal injuries (eg. fibrosis) (94). Introduction of lyophilization and powdering as an alternative way of tissue preparation is proven to be a potential solution for strongly disperse data caused by inhomogeneous injury. Our experiments revealed that protein and RNA isolation performed from a small portion of pulverized tissue results in lower scatter, than from segmented parts of frozen samples. These findings verified our hypothesis that lyophilization and powdering of fibrotic tissues improve the reproducibility of molecular biological measurements.

Although, the majority of biological samples are generally stored frozen at -80°C to preserve liable components such as proteins and nucleic acids, there are several disadvantages to be considered. Due to the limited storage capacity, research laboratories usually require several ultra-low temperature freezers, which generates significant amount of heat and CO_2 in addition to high operating costs. Another drawback of frozen storage is sample thawing, to which biochemical substances are extremely sensitive. However, inconvenient shipping is the most frequently reported issue, particularly due to the cold chain transportation and safety concerns of liquid nitrogen tanks.

To implicate an alternative method for storing and preprocessing of highly valuable biological specimens, it is essential to validate its safety and reliability. The majority of studies show that properly executed freeze-drying followed by short- or mid-term storage does not impair RNA and protein content (95–97). Consequently, we demonstrated that lyophilization followed by long-term storage (20 months) at 4°C does not decrease the

levels of the investigated molecules including the highly sensitive post-translation modifications such as phosphorylation.

The role of lyophilization in the food- and pharmaceutical industry has continuously increased over the last decades, and currently, it is gaining space in clinical research as well (98,99). The interpretation of PD effluent as a “liquid biopsy” used for detecting biomarkers of pathological processes, such as the development of peritoneal fibrosis has become an emerging topic in clinical research. Peritoneal fibrosis is associated with fibrous thickening of the peritoneum caused by various pathological conditions related to clinical practices such as peritoneal dialysis (100). Pro-fibrotic markers, such as CTGF levels of PD effluent may provide valuable information about disease progression, in addition, non-invasive sampling allows continuous monitoring (101). However, detection of biomarker proteins in PD effluent with Western blotting is challenging due to their low concentration. Following 20x concentration of PD by lyophilization and rehydration we were able to detect CTGF, demonstrating that freeze-drying is a potential method to enrich proteins with low abundance but high clinical significance.

Another rapidly evolving field is metabolome research which is addressed to get deeper understanding in role of the human gut microbiome to enlighten its therapeutic potential. Lyophilization has already been incorporated as a useful tool for removing liquid components from the feces before fecal microbiota transplantation, which is a promising concept in the treatment of gastrointestinal diseases (102,103). Metabolomics also uses highly sensitive analytical tools like high-performance liquid chromatography – mass spectrometry (HPLC-MS) which require pure, solvent free samples (104). Although, the convenience of drying feces by lyophilization has been proven, there are no comprehensive freeze-drying setups available. We published a detailed protocol which results in solvent free product without deteriorating the composition of stool samples. Metabolite analysis revealed that lyophilization results higher number and concentration of detected substances belonging to various classes in comparison with the commercially available sample preparation kit.

DOI:10.14753/SE.2023.2872

6. Conclusions

1. Novel urinary biomarkers of collagen turnover are able to detect diabetes induced kidney fibrosis.
2. Evaluation of focal tissue damage (eg. fibrosis) usually results in highly disperse data due to suboptimal sampling.
3. Freeze-drying and powdering fibrotic tissues increase the precision of molecular biological measurements including RT-qPCR and Western blot.
4. Lyophilized samples can be permanently stored at 4°C without the degradation of RNA and protein content, and post-translational modifications.
5. Lyophilization is a suitable method for concentrating highly valuable biological specimens such as PD effluent and preserving protein content.
6. Water removal by freeze-drying results in higher number and concentration of substances detected in human fecal samples compared to conventional preprocessing.

DOI:10.14753/SE.2023.2872

7. Summary

Diabetic kidney disease (DKD) is a global burden affecting 30-40% of diabetic patients. The risk of morbidity and mortality are unacceptably high, thereby, early initiation of an effective therapy is crucial to prevent or slow down the progression of renal complications. However, currently there is no appropriate biomarker of DKD, which makes diagnosis challenging. In this work we tested novel urinary biomarkers of kidney fibrosis, an advanced manifestation of the disease.

Urinary levels of N-terminal type III collagen propeptide, collagen type III breakdown product and tumstatin indicated the presence of diabetes induced kidney fibrosis. Although, renal parameters and histological evaluations showed significant improvement in animals that received RAAS inhibitor treatment, urinary markers of collagen turnover did not reflect these alterations.

In line with previous results, this experiment resulted in highly disperse data due to the focal nature of tissue fibrosis. Therefore, we developed a lyophilization sample preprocessing method to tackle this problem. Following setting up applicable freeze-drying protocols for various biological specimens (rat kidney, heart, lungs; human peritoneal dialysis effluent and feces) we confirmed our hypothesis that powdering lyophilized tissues provides homogeneous samples and improves the precision of qualitative and quantitative measurements. We also verified the method by demonstrating that freeze-drying preserves RNA and protein content, and post-translational modifications such as phosphorylation even after long-term (20 months) storage at 4°C. Furthermore, lyophilization is proven to be suitable for removing water from highly valuable human samples such as peritoneal dialysis effluent and fecal samples without the degradation of low-abundance proteins and other substances.

In conclusion, urinary biomarkers of extracellular matrix formation can indicate diabetes induced kidney fibrosis at the early stage, however, their sensitivity may be insufficient to monitor therapeutic improvement. Beyond the extended and more convenient storability, lyophilization should also be considered as a superior alternative method of biological sample preprocessing to achieve higher reproducibility, better product quality and more reliable results. Freeze-drying conceals yet untapped opportunities which are worth utilizing in the basic- and clinical research as well.

8. References

1. Kovesdy CP. Epidemiology of chronic kidney disease: an update 2022. Kidney Int Suppl [Internet]. 2022 Apr 1 [cited 2023 Apr 4];12(1):7. Available from: /pmc/articles/PMC9073222/

2. Mills KT, Xu Y, Zhang W, Bundy JD, Chen CS, Kelly TN, et al. A systematic analysis of worldwide population-based data on the global burden of chronic kidney disease in 2010. Kidney Int [Internet]. 2015 Nov 1 [cited 2023 Apr 4];88(5):950–7. Available from: https://pubmed.ncbi.nlm.nih.gov/26221752/

3. Bello AK, Levin A, Lunney M, Osman MA, Ye F, Ashuntantang GE, et al. Status of care for end stage kidney disease in countries and regions worldwide: international cross sectional survey. BMJ [Internet]. 2019 Oct 31 [cited 2023 Apr 5];367:38. Available from: https://www.bmj.com/content/367/bmj.l5873

4. Thomas MC, Brownlee M, Susztak K, Sharma K, Jandeleit-Dahm KAM, Zoungas S, et al. Diabetic kidney disease. Nat Rev Dis Prim 2015 11 [Internet]. 2015 Jul 30 [cited 2023 Apr 4];1(1):1–20. Available from: https://www.nature.com/articles/nrdp201518

5. Thomas MC, Weekes AJ, Broadley OJ, Cooper ME, Mathew TH. The burden of chronic kidney disease in Australian patients with type 2 diabetes (the NEFRON study). Med J Aust [Internet]. 2006 Aug 7 [cited 2023 Apr 4];185(3):140–4. Available from: https://appserver-3691d15a-nginx-64ff5a5077f040e582d9d907cb6e0557/journal/2006/185/3/burden-chronic-kidney-disease-australian-patients-type-2-diabetes-nefron-study

6. Dwyer JP, Parving H-H, Hunsicker LG, Ravid M, Remuzzi G, Lewis JB. Renal Dysfunction in the Presence of Normoalbuminuria in Type 2 Diabetes: Results from the DEMAND Study. Cardiorenal Med [Internet]. 2012 [cited 2023 Apr 4];2(1):1–10. Available from: https://pubmed.ncbi.nlm.nih.gov/22493597/

7. Arya A, Aggarwal S, Yadav HN. Pathogenesis of Diabetic Nephropathy. Int J Pharm Pharm Sci [Internet]. 2021 Nov [cited 2023 Apr 4];2(SUPPL. 4):24–9. Available from: https://www.ncbi.nlm.nih.gov/books/NBK571720/

8. Amorim RG, Guedes G da S, Vasconcelos SM de L, Santos JC de F. Kidney Disease in Diabetes Mellitus: Cross-Linking between Hyperglycemia, Redox Imbalance and Inflammation. Arq Bras Cardiol [Internet]. 2019 May 1 [cited 2023 Apr 4];112(5):577–87. Available from: https://pubmed.ncbi.nlm.nih.gov/31188964/

9. Donate-Correa J, Martín-Núñez E, Muros-De-Fuentes M, Mora-Fernández C, Navarro-González JF. Inflammatory cytokines in diabetic nephropathy. J Diabetes Res [Internet]. 2015 [cited 2023 Apr 4];2015. Available from: https://pubmed.ncbi.nlm.nih.gov/25785280/

10. Arsov S, Graaff R, Van Oeveren W, Stegmayr B, Sikole A, Rakhorst G, et al. Advanced glycation end-products and skin autofluorescence in end-stage renal disease: a review. Clin Chem Lab Med [Internet]. 2014 Jan 1 [cited 2023 Apr 4];52(1):11–20. Available from: https://pubmed.ncbi.nlm.nih.gov/23612551/

11. Geraldes P, King GL. Activation of protein kinase C isoforms and its impact on diabetic complications. Circ Res [Internet]. 2010 Apr 30 [cited 2023 Apr 4];106(8):1319–31. Available from: https://pubmed.ncbi.nlm.nih.gov/20431074/

12. Stinghen AEM, Massy ZA, Vlassara H, Striker GE, Boullier A. Uremic Toxicity of Advanced Glycation End Products in CKD. J Am Soc Nephrol [Internet]. 2016 Feb 1 [cited 2023 Apr 4];27(2):354–70. Available from: https://pubmed.ncbi.nlm.nih.gov/26311460/

13. Matsui T, Higashimoto Y, Nishino Y, Nakamura N, Fukami K, Yamagishi SI. RAGE-Aptamer Blocks the Development and Progression of Experimental Diabetic Nephropathy. Diabetes [Internet]. 2017 Jun 1 [cited 2023 Apr 4];66(6):1683–95. Available from: https://pubmed.ncbi.nlm.nih.gov/28385802/

14. Jeong BY, Uddin MJ, Park JH, Lee JH, Lee HB, Miyata T, et al. Novel Plasminogen Activator Inhibitor-1 Inhibitors Prevent Diabetic Kidney Injury in a Mouse Model. PLoS One [Internet]. 2016 Jun 1 [cited 2023 Apr 5];11(6). Available from: /pmc/articles/PMC4892642/

15. Carmines PK. The Renal Vascular Response to Diabetes. Curr Opin Nephrol Hypertens [Internet]. 2010 Jan [cited 2023 Apr 4];19(1):85. Available from:

/pmc/articles/PMC2886724/

16. Lim AKH. Diabetic nephropathy - complications and treatment. Int J Nephrol Renovasc Dis [Internet]. 2014 Oct 15 [cited 2023 Apr 4];7:361–81. Available from: https://pubmed.ncbi.nlm.nih.gov/25342915/

17. Bakris GL. Recognition, Pathogenesis, and Treatment of Different Stages of Nephropathy in Patients With Type 2 Diabetes Mellitus. Mayo Clin Proc [Internet]. 2011 [cited 2023 Apr 4];86(5):444. Available from: /pmc/articles/PMC3084647/

18. Fine LG, Orphanides C NJ. Progressive renal disease: the chronic hypoxia hypothesis. Kidney Int Suppl. 1998;65(S74-8).

19. Kang DH, Kanellis J, Hugo C, Truong L, Anderson S, Kerjaschki D, et al. Role of the microvascular endothelium in progressive renal disease. J Am Soc Nephrol [Internet]. 2002 [cited 2023 Apr 4];13(3):806–16. Available from: https://pubmed.ncbi.nlm.nih.gov/11856789/

20. Basile DP, Donohoe D, Roethe K, Osborn JL. Renal ischemic injury results in permanent damage to peritubular capillaries and influences long-term function. Am J Physiol Renal Physiol [Internet]. 2001 Nov [cited 2023 Apr 4];281(5):F887–99. Available from: https://pubmed.ncbi.nlm.nih.gov/11592947/

21. Bohle A, Mackensen-Haen S, Wehrmann M. Significance of postglomerular capillaries in the pathogenesis of chronic renal failure. Kidney Blood Press Res [Internet]. 1996 [cited 2023 Apr 4];19(3–4):191–5. Available from: https://pubmed.ncbi.nlm.nih.gov/8887259/

22. Ferenbach DA, Bonventre J V. Mechanisms of maladaptive repair after AKI leading to accelerated kidney ageing and CKD. Nat Rev Nephrol [Internet]. 2015 May 30 [cited 2023 Apr 4];11(5):264–76. Available from: https://pubmed.ncbi.nlm.nih.gov/25643664/

23. Yang L, Besschetnova TY, Brooks CR, Shah J V., Bonventre J V. Epithelial cell cycle arrest in G2/M mediates kidney fibrosis after injury. Nat Med [Internet]. 2010 May [cited 2023 Apr 4];16(5):535–43. Available from:

https://pubmed.ncbi.nlm.nih.gov/20436483/

24. Canaud G, Bonventre J V. Cell cycle arrest and the evolution of chronic kidney disease from acute kidney injury. Nephrol Dial Transplant [Internet]. 2015 Apr 1 [cited 2023 Apr 4];30(4):575–83. Available from: https://pubmed.ncbi.nlm.nih.gov/25016609/

25. Basile DP. The endothelial cell in ischemic acute kidney injury: implications for acute and chronic function. Kidney Int [Internet]. 2007 Jul [cited 2023 Apr 4];72(2):151–6. Available from: https://pubmed.ncbi.nlm.nih.gov/17495858/

26. Kwon O, Hong SM, Sutton TA, Temm CJ. Preservation of peritubular capillary endothelial integrity and increasing pericytes may be critical to recovery from postischemic acute kidney injury. Am J Physiol Renal Physiol [Internet]. 2008 [cited 2023 Apr 4];295(2). Available from: https://pubmed.ncbi.nlm.nih.gov/18562634/

27. Yamanouchi M, Furuichi K, Hoshino J, Ubara Y, Wada T. Nonproteinuric diabetic kidney disease. Clin Exp Nephrol [Internet]. 2020 Jul 1 [cited 2023 Apr 5];24(7):573. Available from: /pmc/articles/PMC7271053/

28. Genovese F, Manresa AA, Leeming DJ, Karsdal MA, Boor P. The extracellular matrix in the kidney: a source of novel non-invasive biomarkers of kidney fibrosis? Fibrogenes Tissue Repair 2014 71 [Internet]. 2014 Mar 28 [cited 2023 Apr 4];7(1):1–14. Available from: https://fibrogenesis.biomedcentral.com/articles/10.1186/1755-1536-7-4

29. Genovese F, Boor P, Papasotiriou M, Leeming DJ, Karsdal MA, Floege J. Turnover of type III collagen reflects disease severity and is associated with progression and microinflammation in patients with IgA nephropathy. Nephrol Dial Transplant [Internet]. 2016 Mar 1 [cited 2023 Apr 4];31(3):472–9. Available from: https://pubmed.ncbi.nlm.nih.gov/26311218/

30. Nielsen SH, Willumsen N, Brix S, Sun S, Manon-Jensen T, Karsdal M, et al. Tumstatin, a Matrikine Derived from Collagen Type IVα3, is Elevated in Serum from Patients with Non-Small Cell Lung Cancer. Transl Oncol [Internet]. 2018 Apr 1 [cited 2023 Apr 4];11(2):528–34. Available from:

https://pubmed.ncbi.nlm.nih.gov/29524830/

31. Papasotiriou M, Genovese F, Klinkhammer BM, Kunter U, Nielsen SH, Karsdal MA, et al. Serum and urine markers of collagen degradation reflect renal fibrosis in experimental kidney diseases. Nephrol Dial Transplant [Internet]. 2015 Jul 1 [cited 2023 Apr 4];30(7):1112–21. Available from: https://academic.oup.com/ndt/article/30/7/1112/2324891

32. Dower K, Zhao S, Schlerman FJ, Savary L, Campanholle G, Johnson BG, et al. High resolution molecular and histological analysis of renal disease progression in ZSF1 fa/faCP rats, a model of type 2 diabetic nephropathy. Joles JA, editor. PLoS One [Internet]. 2017 Jul 26 [cited 2023 Apr 4];12(7):e0181861. Available from: https://pubmed.ncbi.nlm.nih.gov/28746409/

33. Ruggenenti P, Fassi A, Ilieva AP, Bruno S, Iliev IP, Brusegan V, et al. Preventing microalbuminuria in type 2 diabetes. N Engl J Med [Internet]. 2004 Nov 4 [cited 2023 Apr 10];351(19):1941–51. Available from: https://pubmed.ncbi.nlm.nih.gov/15516697/

34. A P, S M, J C, B N, M W, L B, et al. Effects of a fixed combination of perindopril and indapamide on macrovascular and microvascular outcomes in patients with type 2 diabetes mellitus (the ADVANCE trial): a randomised controlled trial. Lancet (London, England) [Internet]. 2007 Sep 8 [cited 2023 Apr 10];370(9590):829–40. Available from: https://pubmed.ncbi.nlm.nih.gov/17765963/

35. Mauer M, Zinman B, Gardiner R, Suissa S, Sinaiko A, Strand T, et al. Renal and retinal effects of enalapril and losartan in type 1 diabetes. N Engl J Med [Internet]. 2009 Jul 2 [cited 2023 Apr 10];361(1):40–51. Available from: https://pubmed.ncbi.nlm.nih.gov/19571282/

36. Gerstein HC, Yusuf S, Mann JFE, Hoogwerf B, Zinman B, Held C, et al. Effects of ramipril on cardiovascular and microvascular outcomes in people with diabetes mellitus: Results of the HOPE study and MICRO-HOPE substudy. Lancet [Internet]. 2000 Jan 22 [cited 2023 Apr 10];355(9200):253–9. Available from: http://www.thelancet.com/article/S0140673699123237/fulltext

37. Imai E, Chan JCN, Ito S, Yamasaki T, Kobayashi F, Haneda M, et al. Effects of olmesartan on renal and cardiovascular outcomes in type 2 diabetes with overt nephropathy: a multicentre, randomised, placebo-controlled study. Diabetologia [Internet]. 2011 Dec [cited 2023 Apr 10];54(12):2978–86. Available from: https://pubmed.ncbi.nlm.nih.gov/21993710/

38. Kobori H, Mori H, Masaki T, Nishiyama A. Angiotensin II blockade and renal protection. Curr Pharm Des [Internet]. 2013 Apr 8 [cited 2023 Apr 10];19(17):3033–42. Available from: https://pubmed.ncbi.nlm.nih.gov/23176216/

39. Fiordaliso F, Cuccovillo I, Bianchi R, Bai A, Doni M, Salio M, et al. Cardiovascular oxidative stress is reduced by an ACE inhibitor in a rat model of streptozotocin-induced diabetes. Life Sci [Internet]. 2006 Jun 6 [cited 2023 Apr 10];79(2):121–9. Available from: https://pubmed.ncbi.nlm.nih.gov/16445948/

40. Gellai R, Hodrea J, Lenart L, Hosszu A, Koszegi S, Balogh D, et al. Role of O-linked N-acetylglucosamine modification in diabetic nephropathy. Am J Physiol Renal Physiol [Internet]. 2016 Dec 1 [cited 2023 Apr 10];311(6):F1172–81. Available from: https://pubmed.ncbi.nlm.nih.gov/27029430/

41. Fan Q, Liao J, Kobayashi M, Yamashita M, Gu L, Gohda T, et al. Candesartan reduced advanced glycation end-products accumulation and diminished nitro-oxidative stress in type 2 diabetic KK/Ta mice. Nephrol Dial Transplant. 2004 Dec;19(12):3012–20.

42. Han KH, Kang YS, Han SY, Jee YH, Lee MH, Han JY, et al. Spironolactone ameliorates renal injury and connective tissue growth factor expression in type II diabetic rats. Kidney Int [Internet]. 2006 Jul 12 [cited 2023 Apr 10];70(1):111–20. Available from: https://pubmed.ncbi.nlm.nih.gov/16723984/

43. Feldman DL, Jin L, Xuan H, Contrepas A, Zhou Y, Webb RL, et al. Effects of aliskiren on blood pressure, albuminuria, and (pro)renin receptor expression in diabetic TG(mRen-2)27 rats. Hypertens (Dallas, Tex 1979) [Internet]. 2008 Jul 1 [cited 2023 Apr 10];52(1):130–6. Available from: https://pubmed.ncbi.nlm.nih.gov/18490518/

44. Holman RR, Paul SK, Bethel MA, Matthews DR, Neil HAW. 10-year follow-up of intensive glucose control in type 2 diabetes. N Engl J Med [Internet]. 2008 Oct 9 [cited 2023 Apr 10];359(15):1577–89. Available from: https://pubmed.ncbi.nlm.nih.gov/18784090/

45. Dekkers CCJ, Petrykiv S, Laverman GD, Cherney DZ, Gansevoort RT, Heerspink HJL. Effects of the SGLT-2 inhibitor dapagliflozin on glomerular and tubular injury markers. Diabetes Obes Metab [Internet]. 2018 Aug 1 [cited 2023 Apr 10];20(8):1988–93. Available from: https://pubmed.ncbi.nlm.nih.gov/29573529/

46. Panchapakesan U, Pegg K, Gross S, Komala MG, Mudaliar H, Forbes J, et al. Effects of SGLT2 inhibition in human kidney proximal tubular cells--renoprotection in diabetic nephropathy? PLoS One [Internet]. 2013 Feb 4 [cited 2023 Apr 10];8(2). Available from: https://pubmed.ncbi.nlm.nih.gov/23390498/

47. Sano M, Takei M, Shiraishi Y, Suzuki Y. Increased Hematocrit During Sodium-Glucose Cotransporter 2 Inhibitor Therapy Indicates Recovery of Tubulointerstitial Function in Diabetic Kidneys. J Clin Med Res [Internet]. 2016 [cited 2023 Apr 10];8(12):844–7. Available from: https://pubmed.ncbi.nlm.nih.gov/27829948/

48. Castoldi G, Carletti R, Ippolito S, Colzani M, Barzaghi F, Stella A, et al. Sodium-glucose cotransporter 2 inhibition prevents renal fibrosis in cyclosporine nephropathy. Acta Diabetol [Internet]. 2021 Aug 1 [cited 2023 Apr 10];58(8):1059–70. Available from: https://pubmed.ncbi.nlm.nih.gov/33760995/

49. Goldstein SL, Devarajan P. PROGRESSION FROM ACUTE KIDNEY INJURY TO CHRONIC KIDNEY DISEASE: A PEDIATRIC PERSPECTIVE: An invited review for Advances in Chronic Kidney Disease. Adv Chronic Kidney Dis [Internet]. 2008 Jul [cited 2023 Apr 4];15(3):278. Available from: /pmc/articles/PMC2481383/

50. Sinha R, Nandi M, Tullus K, Marks SD, Taraphder A. Ten-year follow-up of children after acute renal failure from a developing country. Nephrol Dial Transplant [Internet]. 2009 Mar [cited 2023 Apr 4];24(3):829–33. Available

from: https://pubmed.ncbi.nlm.nih.gov/18852189/

51. Askenazi DJ, Feig DI, Graham NM, Hui-Stickle S, Goldstein SL. 3-5 year longitudinal follow-up of pediatric patients after acute renal failure. Kidney Int [Internet]. 2006 Jan [cited 2022 Oct 3];69(1):184–9. Available from: https://pubmed.ncbi.nlm.nih.gov/16374442/

52. Hsu RK, Hsu C yuan. THE ROLE OF ACUTE KIDNEY INJURY IN CHRONIC KIDNEY DISEASE. Semin Nephrol [Internet]. 2016 Jul 1 [cited 2023 Apr 4];36(4):283. Available from: /pmc/articles/PMC4979984/

53. Schnaper HW. Remnant nephron physiology and the progression of chronic kidney disease. Pediatr Nephrol [Internet]. 2014 Feb [cited 2023 Apr 4];29(2):193–202. Available from: /pmc/articles/PMC3796124/

54. Luyckx VA, Tonelli M, Stanifer JW. The global burden of kidney disease and the sustainable development goals. Bull World Health Organ [Internet]. 2018 Jun 6 [cited 2023 Apr 4];96(6):414. Available from: /pmc/articles/PMC5996218/

55. Olowu WA, Niang A, Osafo C, Ashuntantang G, Arogundade FA, Porter J, et al. Outcomes of acute kidney injury in children and adults in sub-Saharan Africa: a systematic review. Lancet Glob Heal [Internet]. 2016 Apr 1 [cited 2023 Apr 4];4(4):e242–50. Available from: https://pubmed.ncbi.nlm.nih.gov/27013312/

56. Susantitaphong P, Cruz DN, Cerda J, Abulfaraj M, Alqahtani F, Koulouridis I, et al. World incidence of AKI: a meta-analysis. Clin J Am Soc Nephrol [Internet]. 2013 [cited 2023 Apr 4];8(9):1482–93. Available from: https://pubmed.ncbi.nlm.nih.gov/23744003/

57. Lameire N, Van Biesen W, Vanholder R. The changing epidemiology of acute renal failure. Nat Clin Pract Nephrol [Internet]. 2006 Jul [cited 2023 Apr 4];2(7):364–77. Available from: https://pubmed.ncbi.nlm.nih.gov/16932465/

58. Bonventre J V., Yang L. Cellular pathophysiology of ischemic acute kidney injury. J Clin Invest [Internet]. 2011 Nov 11 [cited 2023 Apr 4];121(11):4210. Available from: /pmc/articles/PMC3204829/

59. Zimmerhackl B, Robertson CR, Jamison RL. The microcirculation of the renal

medulla. Circ Res [Internet]. 1985 [cited 2023 Apr 4];57(5):657–67. Available from: https://pubmed.ncbi.nlm.nih.gov/3902277/

60. Crislip GR, O'Connor PM, Wei Q, Sullivan JC. Vasa recta pericyte density is negatively associated with vascular congestion in the renal medulla following ischemia reperfusion in rats. Am J Physiol Renal Physiol [Internet]. 2017 Nov 29 [cited 2023 Apr 4];313(5):F1097–105. Available from: https://pubmed.ncbi.nlm.nih.gov/28794065/

61. Hanif MO, Bali A, Ramphul K. Acute Renal Tubular Necrosis. StatPearls [Internet]. 2023 Feb 19 [cited 2023 Apr 8]; Available from: https://www.ncbi.nlm.nih.gov/books/NBK507815/

62. Yuan Q, Tan RJ, Liu Y. Myofibroblast in Kidney Fibrosis: Origin, Activation, and Regulation. Adv Exp Med Biol [Internet]. 2019 [cited 2023 Jun 6];1165:253–83. Available from: https://pubmed.ncbi.nlm.nih.gov/31399969/

63. Quaggin SE, Kapus A. Scar wars: mapping the fate of epithelial-mesenchymal-myofibroblast transition. Kidney Int [Internet]. 2011 [cited 2023 Jun 6];80(1):41–50. Available from: https://pubmed.ncbi.nlm.nih.gov/21430641/

64. Chen YT, Chang FC, Wu CF, Chou YH, Hsu HL, Chiang WC, et al. Platelet-derived growth factor receptor signaling activates pericyte-myofibroblast transition in obstructive and post-ischemic kidney fibrosis. Kidney Int [Internet]. 2011 [cited 2023 Jun 6];80(11):1170–81. Available from: https://pubmed.ncbi.nlm.nih.gov/21716259/

65. Lin SL, Kisseleva T, Brenner DA, Duffield JS. Pericytes and perivascular fibroblasts are the primary source of collagen-producing cells in obstructive fibrosis of the kidney. Am J Pathol [Internet]. 2008 [cited 2023 Jun 6];173(6):1617–27. Available from: https://pubmed.ncbi.nlm.nih.gov/19008372/

66. Kramann R, Schneider RK, Dirocco DP, Machado F, Fleig S, Bondzie PA, et al. Perivascular Gli1+ progenitors are key contributors to injury-induced organ fibrosis. Cell Stem Cell [Internet]. 2015 Jan 8 [cited 2023 Jun 6];16(1):51–66. Available from: https://pubmed.ncbi.nlm.nih.gov/25465115/

67. Li L, Fu H, Liu Y. The fibrogenic niche in kidney fibrosis: components and mechanisms. Nat Rev Nephrol [Internet]. 2022 Sep 1 [cited 2023 Jun 6];18(9):545–57. Available from: https://pubmed.ncbi.nlm.nih.gov/35788561/

68. Rey L, editor. Freeze-Drying/Lyophilization of Pharmaceutical and Biological Products [Internet]. CRC Press; 2016 [cited 2023 Apr 8]. Available from: https://www.taylorfrancis.com/books/9781439825761

69. Wang W. Lyophilization and development of solid protein pharmaceuticals. Int J Pharm [Internet]. 2000 Aug 1 [cited 2023 Apr 4];203(1–2):1–60. Available from: https://pubmed.ncbi.nlm.nih.gov/10967427/

70. A significant comparison between collapse and glass transition temperatures - European Pharmaceutical Review [Internet]. 2008 [cited 2023 Apr 8]. Available from: https://www.europeanpharmaceuticalreview.com/article/1479/a-significant-comparison-between-collapse-and-glass-transition-temperatures/

71. Yu L. Amorphous pharmaceutical solids: preparation, characterization and stabilization. Adv Drug Deliv Rev. 2001 May 16;48(1):27–42.

72. Rathore AS, Bhambure R, Ghare V. Process analytical technology (PAT) for biopharmaceutical products. Anal Bioanal Chem 2010 3981 [Internet]. 2010 May 18 [cited 2023 Apr 8];398(1):137–54. Available from: https://link.springer.com/article/10.1007/s00216-010-3781-x

73. Sharma D. Design Space Development for Lyophilization Using DOE and Process Modeling. BioPharm Int [Internet]. 2010 Apr 28 [cited 2023 Apr 4];23(9):40–45–40–45. Available from: https://www.biopharminternational.com/view/design-space-development-lyophilization-using-doe-and-process-modeling

74. Giordano A, Barresi AA, Fissore D. On the use of mathematical models to build the design space for the primary drying phase of a pharmaceutical lyophilization process. J Pharm Sci [Internet]. 2011 [cited 2023 Apr 4];100(1):311–24. Available from: https://pubmed.ncbi.nlm.nih.gov/20575053/

75. Sundaramurthi P, Suryanarayanan R. Calorimetry and complementary techniques

to characterize frozen and freeze-dried systems. Adv Drug Deliv Rev [Internet]. 2012 Apr [cited 2023 Apr 4];64(5):384–95. Available from: https://pubmed.ncbi.nlm.nih.gov/22210136/

76. Horn J, Friess W. Detection of collapse and crystallization of saccharide, protein, and mannitol formulations by optical fibers in lyophilization. Front Chem. 2018 Jan 26;6(JAN):4.

77. Nail S, Tchessalov S, Shalaev E, Ganguly A, Renzi E, Dimarco F, et al. Recommended Best Practices for Process Monitoring Instrumentation in Pharmaceutical Freeze Drying-2017. AAPS PharmSciTech [Internet]. 2017 Oct 1 [cited 2023 Apr 8];18(7):2379–93. Available from: https://pubmed.ncbi.nlm.nih.gov/28205144/

78. Wu Y, Wu M, Zhang Y, Li W, Gao Y, Li Z, et al. Lyophilization is suitable for storage and shipment of fresh tissue samples without altering RNA and protein levels stored at room temperature. Amino Acids [Internet]. 2012 Sep [cited 2023 Apr 4];43(3):1383–8. Available from: https://pubmed.ncbi.nlm.nih.gov/22215254/

79. Bircher L, Geirnaert A, Hammes F, Lacroix C, Schwab C. Effect of cryopreservation and lyophilization on viability and growth of strict anaerobic human gut microbes. Microb Biotechnol [Internet]. 2018 Jul 1 [cited 2023 Apr 4];11(4):721–33. Available from: https://pubmed.ncbi.nlm.nih.gov/29663668/

80. Bossi R de L, Cabral M, Oliveira M, Lopes S, Hurtado R, Sampaio M, et al. Ultrastructural analysis of Lyophilized Human Spermatozoa. JBRA Assist Reprod [Internet]. 2021 [cited 2023 Apr 4];25(3):473–9. Available from: https://pubmed.ncbi.nlm.nih.gov/34286941/

81. Mocchi M, Bari E, Marrubini G, Bonda AF, Perteghella S, Tartara F, et al. Freeze-Dried Mesenchymal Stem Cell-Secretome Pharmaceuticalization: Optimization of Formulation and Manufacturing Process Robustness. Pharmaceutics [Internet]. 2021 Aug 1 [cited 2023 Apr 4];13(8). Available from: https://pubmed.ncbi.nlm.nih.gov/34452088/

82. Tavar E, Turk E, Kreft S. Simple Modification of Karl-Fischer Titration Method

for Determination of Water Content in Colored Samples. J Anal Methods Chem [Internet]. 2012 [cited 2023 Apr 8];2012(1). Available from: /pmc/articles/PMC3335423/

83. Genovese F, Rasmussen DGK, Karsdal MA, Jesky M, Fenton A, Cockwell P. Imbalanced turnover of collagen type III is associated with disease progression and mortality in high-risk chronic kidney disease patients. Clin Kidney J [Internet]. 2021 Feb 16 [cited 2023 Apr 8];14(2):593–601. Available from: https://academic.oup.com/ckj/article/14/2/593/5704451

84. Neprasova M, Maixnerova D, Sparding N, Genovese F, Karsdal MA, Koprivova H, et al. Serum and Urine Biomarkers Related to Kidney Fibrosis Predict Kidney Outcome in Czech Patients with IgA Nephropathy. Int J Mol Sci 2023, Vol 24, Page 2064 [Internet]. 2023 Jan 20 [cited 2023 Apr 8];24(3):2064. Available from: https://www.mdpi.com/1422-0067/24/3/2064/htm

85. Poulsen CG, Rasmussen DGK, Genovese F, Hansen TW, Nielsen SH, Reinhard H, et al. Marker for kidney fibrosis is associated with inflammation and deterioration of kidney function in people with type 2 diabetes and microalbuminuria. PLoS One [Internet]. 2023 Mar 17 [cited 2023 Apr 8];18(3):e0283296. Available from: https://pubmed.ncbi.nlm.nih.gov/36930632/

86. Genovese F, Akhgar A, Lim SS, Farris AB, Battle M, Cobb J, et al. Collagen Type III and VI Remodeling Biomarkers Are Associated with Kidney Fibrosis in Lupus Nephritis. Kidney360 [Internet]. 2021 Sep 9 [cited 2023 Apr 8];2(9):1473. Available from: /pmc/articles/PMC8786137/

87. Merivaara A, Zini J, Koivunotko E, Valkonen S, Korhonen O, Fernandes FM, et al. Preservation of biomaterials and cells by freeze-drying: Change of paradigm. J Control Release. 2021 Aug 10;336:480–98.

88. Carpentier SC, Dens K, Van Den Houwe I, Swennen R, Panis B. Lyophilization, a Practical Way to Store and Transport Tissues Prior to Protein Extraction for 2DE Analysis? Proteomics [Internet]. 2007 Sep 1 [cited 2023 Apr 8];7(S1):64–9. Available from: https://onlinelibrary.wiley.com/doi/full/10.1002/pmic.200700529

89. García-Baldenegro CV, Vargas-Arispuro I, Islas-Osuna M, Rivera-Domínguez M, Aispuro-Hernández E, Martínez-Tíllez M íngel. Total RNA quality of lyophilized and cryopreserved dormant grapevine buds. Electron J Biotechnol. 2015 Mar 1;18(2):134–7.

90. Gill P, Moghadam TT, Ranjbar B. Differential Scanning Calorimetry Techniques: Applications in Biology and Nanoscience. J Biomol Tech [Internet]. 2010 Dec [cited 2023 Apr 8];21(4):167. Available from: /pmc/articles/PMC2977967/

91. Alonso-García T, Rodríguez-Presa MJ, Gervasi C, Moya S, Azzaroni O. Electrochemical determination of the glass transition temperature of thin polyelectrolyte brushes at solid-liquid interfaces by impedance spectroscopy. Anal Chem [Internet]. 2013 Jul 16 [cited 2023 Apr 8];85(14):6561–5. Available from: https://pubs.acs.org/doi/full/10.1021/ac4007655

92. Ruan RR, Long Z, Song A, Chen PL. Determination of the Glass Transition Temperature of Food Polymers Using Low Field NMR. LWT - Food Sci Technol. 1998 Sep 1;31(6):516–21.

93. He J, Liu W, Huang YX. Simultaneous Determination of Glass Transition Temperatures of Several Polymers. PLoS One [Internet]. 2016 Mar 1 [cited 2023 Apr 8];11(3). Available from: /pmc/articles/PMC4795599/

94. Schipke J, Brandenberger C, Rajces A, Manninger M, Alogna A, Post H, et al. Assessment of cardiac fibrosis: A morphometric method comparison for collagen quantification. J Appl Physiol [Internet]. 2017 [cited 2023 Apr 8];122(4):1019–30. Available from: https://journals.physiology.org/doi/10.1152/japplphysiol.00987.2016

95. Wu Y, Wu M, Zhang Y, Li W, Gao Y, Li Z, et al. Lyophilization is suitable for storage and shipment of fresh tissue samples without altering RNA and protein levels stored at room temperature. Amino Acids [Internet]. 2012 Sep [cited 2023 Apr 8];43(3):1383–8. Available from: https://pubmed.ncbi.nlm.nih.gov/22215254/

96. Damsteegt EL, McHugh N, Lokman PM. Storage by lyophilization - Resulting

RNA quality is tissue dependent. Anal Biochem [Internet]. 2016 Oct 15 [cited 2023 Apr 8];511:92–6. Available from: https://pubmed.ncbi.nlm.nih.gov/27515991/

97. Mareninov S, De Jesus J, Sanchez DE, Kay AB, Wilson RW, Babic I, et al. Lyophilized brain tumor specimens can be used for histologic, nucleic acid, and protein analyses after 1 year of room temperature storage. J Neurooncol [Internet]. 2013 Jul [cited 2023 Apr 8];113(3):365–73. Available from: https://pubmed.ncbi.nlm.nih.gov/23640138/

98. Ribeiro TA, Coussirat C, Pagnussato F, Diesel CV, Macedo FC de S, Macedo CA de S, et al. Lyophilized xenograft: a case series of histological analysis of biopsies. Cell Tissue Bank [Internet]. 2015 Jun 1 [cited 2023 Apr 12];16(2):227–33. Available from: https://pubmed.ncbi.nlm.nih.gov/25168485/

99. Deshmukh AS, Steenberg DE, Hostrup M, Birk JB, Larsen JK, Santos A, et al. Deep muscle-proteomic analysis of freeze-dried human muscle biopsies reveals fiber type-specific adaptations to exercise training. Nat Commun 2021 121 [Internet]. 2021 Jan 12 [cited 2023 Apr 12];12(1):1–15. Available from: https://www.nature.com/articles/s41467-020-20556-8

100. Terri M, Trionfetti F, Montaldo C, Cordani M, Tripodi M, Lopez-Cabrera M, et al. Mechanisms of Peritoneal Fibrosis: Focus on Immune Cells–Peritoneal Stroma Interactions. Front Immunol. 2021 Mar 29;12:235.

101. Sakai N, Nakamura M, Lipson KE, Miyake T, Kamikawa Y, Sagara A, et al. Inhibition of CTGF ameliorates peritoneal fibrosis through suppression of fibroblast and myofibroblast accumulation and angiogenesis. Sci Reports 2017 71 [Internet]. 2017 Jul 14 [cited 2023 Apr 8];7(1):1–13. Available from: https://www.nature.com/articles/s41598-017-05624-2

102. Moosmang S, Pitscheider M, Sturm S, Seger C, Tilg H, Halabalaki M, et al. Metabolomic analysis-Addressing NMR and LC-MS related problems in human feces sample preparation. Clin Chim Acta [Internet]. 2019 Feb 1 [cited 2023 Apr 8];489:169–76. Available from: https://pubmed.ncbi.nlm.nih.gov/29097223/

103. Staley C, Hamilton MJ, Vaughn BP, Graiziger CT, Newman KM, Kabage AJ, et

al. Successful Resolution of Recurrent Clostridium difficile Infection using Freeze-Dried, Encapsulated Fecal Microbiota; Pragmatic Cohort Study. Am J Gastroenterol [Internet]. 2017 Jun 1 [cited 2023 Apr 8];112(6):940–7. Available from: https://pubmed.ncbi.nlm.nih.gov/28195180/

104. Hsu YL, Chen CC, Lin YT, Wu WK, Chang LC, Lai CH, et al. Evaluation and Optimization of Sample Handling Methods for Quantification of Short-Chain Fatty Acids in Human Fecal Samples by GC-MS. J Proteome Res [Internet]. 2019 May 3 [cited 2023 Apr 8];18(5):1948–57. Available from: https://pubmed.ncbi.nlm.nih.gov/30895795/

9. Bibliography of publications

Publications related to the theme of the PhD thesis

Agnes Molnar*, **Tamas Lakat***, Adam Hosszu, Beata Szebeni, Anna Balogh, Laszlo Orfi, Attila J. Szabo, Andrea Fekete, Judit Hodrea; Lyophilization and homogenization of biological samples improves reproducibility and reduces standard deviation in molecular biology techniques. Amino Acids 53, 917-928 2021 **IF=3.789**

Sandor Koszegi, Agnes Molnar, Lilla Lenart, Judit Hodrea, Dora Bianka Balogh, **Tamas Lakat**, Edgar Szkibinszkij, Adam Hosszu, Nadja Sparding, Federica Genovese, Laszlo Wagner, Adam Vannay, Attila J Szabo, Andrea Fekete; RAAS inhibitors directly reduce diabetes-induced renal fibrosis via growth factor inhibition. J Physiol 00.0 pp 1-17 2018 **IF=4.547**

Other publications

Dora Bianka Balogh, Agnes Molnar, Adam Hosszu, **Tamas Lakat**, Judit Hodrea, Attila J. Szabo, Lilla Lenart, Andrea Fekete; Antidepressant effect in diabetes-associated depression: A novel potential of RAAS inhibition. Psychoneuroendocrinology 118:1047005 2020 **IF=4.905**

Lénárt Lilla, **Lakat Tamás**, Hodrea Judit, Fekete Andrea; A renin-angiotenzin-aldoszteron rendszer szerepe a diabéteshez társuló depresszióban. Diabetologia Hungarica 27 : 3pp. 181-187. 7p 2019

DOI:10.14753/SE.2023.2872

10. Acknowledgements

I am profoundly thankful to my supervisor Adam Hosszu for his personal and professional support. I would like to emphasize his contribution to the improvement of my writing and snowboarding skills for which I am deeply grateful.

I would like to express my deep sense of gratitude to Andrea Fekete for giving me the opportunity to be part of MTA-SE Lendület "Momentum" Diabetes Research Group and for continuously supporting me even in the hard times. Her extraordinary dedication was giving me encouragement and helping me to keep motivated.

I wish to sincerely thank Professor Attila Szabo for the privilege to work as a PhD student in the Research Laboratory of the Pediatric Center, Semmelweis University.

I am also very grateful to the post-docs of our group, Dora Bianka Balogh, Judit Hodrea and Lilla Lenart for teaching me the basics and also polishing my research skills. Their experience and insightful suggestions laid the foundation for my professional development.

I would like to thank all my colleagues at the lab for creating a motivating and friendly atmosphere. Special thanks to Agnes Molnar, Akos Toth, Eszter Levai and Csenge Pajtok for the deep discussions and also for having great times together. Without their support and professional help this work could not have been completed. I could not be more thankful to Maria Bernath for help with the laboratory work and for her kind attention on everyone in the lab. I am grateful to Eva Forizs for helping me out with things I could not find. I am privileged and glad of having the fellow and former colleagues as well: Adar Amedi, Minh Tran, Adnan Mohd, Apor Veres-Szekely, Beata Szebeni, Domonkos Pap, Csenge Szasz, Peter Bokrossy, Magdolna Keszthelyi, Violetta Antal, Eszter Javorszky, Daniel Seidl, Regina Legradi, Mate Ketszeri, Istvan Takacs and Ganna Stepanova.

Last but not least, above all special thanks to Timea Medveczki and to my whole family for their enormous support and love I received throughout these years. Thank you for taking a chance on me, and believing in what I could become.